On a Routing Network of Causal Flow and Its Reading under Four-Dimensional Spacetime

C.Y. Hsieh
Rayark Inc.

27 October 2026 [v5]

Abstract

This paper builds a causal network and asks what it can be read as, with four-dimensional spacetime as the frame of the readings. The network is a purely mathematical structure: it stores no coordinate, shared clock or field, and only routes causal flow along ribbons on the Laves graph of a three-torus. The graph is a cubic crystal net, the discrete frame for the symmetries read as CP and CPT. A single irreversible event, the lock, twists every ribbon with one handedness and gives some vertices an extra twist; only at these vertices can flow be held and delayed, and holding gives the network's history an arrow. The routing mixes the flow into a causally trivial medium, the datum of every reading: only what departs from it is nontrivial and can be read. Under coarse-graining the lattice detail of the routing becomes irrelevant and one collective mode survives, isotropic, with a fixed stride in cells per update. Physics enters through readers inside the network, which receive only counts of the flow passed between them and a source. An incidence transform turns the counts into an image on the reader's sky, and demodulation decodes the nontrivial part, carried on phase and frequency channels. Under conventions of scale and of relativity, with light's speed as the conversion ratio between space and time, the decoded signals read as rest mass and gravity, charge and its Coulomb field, and Bose and Fermi statistics. Every claim is graded, from forced to candidate, and since the routing network can be implemented as a finite-state machine, every measured one is checked by released code and records.

Keywords: emergent spacetime; pregeometry; causal network; lattice gas automata; Laves graph; relationalism

1 Introduction

Physics knows space, time and motion only through readings, a clock's ticks or a detector's counts; this paper builds the readings first, with these as their frame. It starts from a causal network that routes causal flow, a purely mathematical structure. The routing machine implements the structure for study; nothing here claims that a machine runs it. The epistemological stance is relationalism: all physics comes from conventional readings over this structure, made by readers within it, with no absolute, objective reader outside the system.

Grades. Every claim in the body carries a grade; the abstract, Section 9's previews and Section 10 carry none. **[F]** forced: no alternative given the principles' working form (Appendix A) and the machine rules; a finite check only if exhaustive; with a named premise, forced given it. **[M]** measured on the machine, or in a model (Appendix C) that the sentence names. **[R]** a reading: a ruled reading of the principles (Appendix A), or a claim holding by a readout convention or the relativity principle (Section 7). **[S]** a declared choice. **[Cond]** a conditional theorem. **[I]** inferred. **[Cand]** a candidate. Grades combine, as in **[F+M]**. A grade covers the claims back to the previous grade or the paragraph's start; a sentence that makes no claim, a definition included, carries none. Fig. 1 maps the trunk of the claims.

The paper has two parts. The causal part (Sections 2–5) is the mathematical structure; its topology supplies the distinguishable degrees of freedom, the signal channels over the causal flow, through

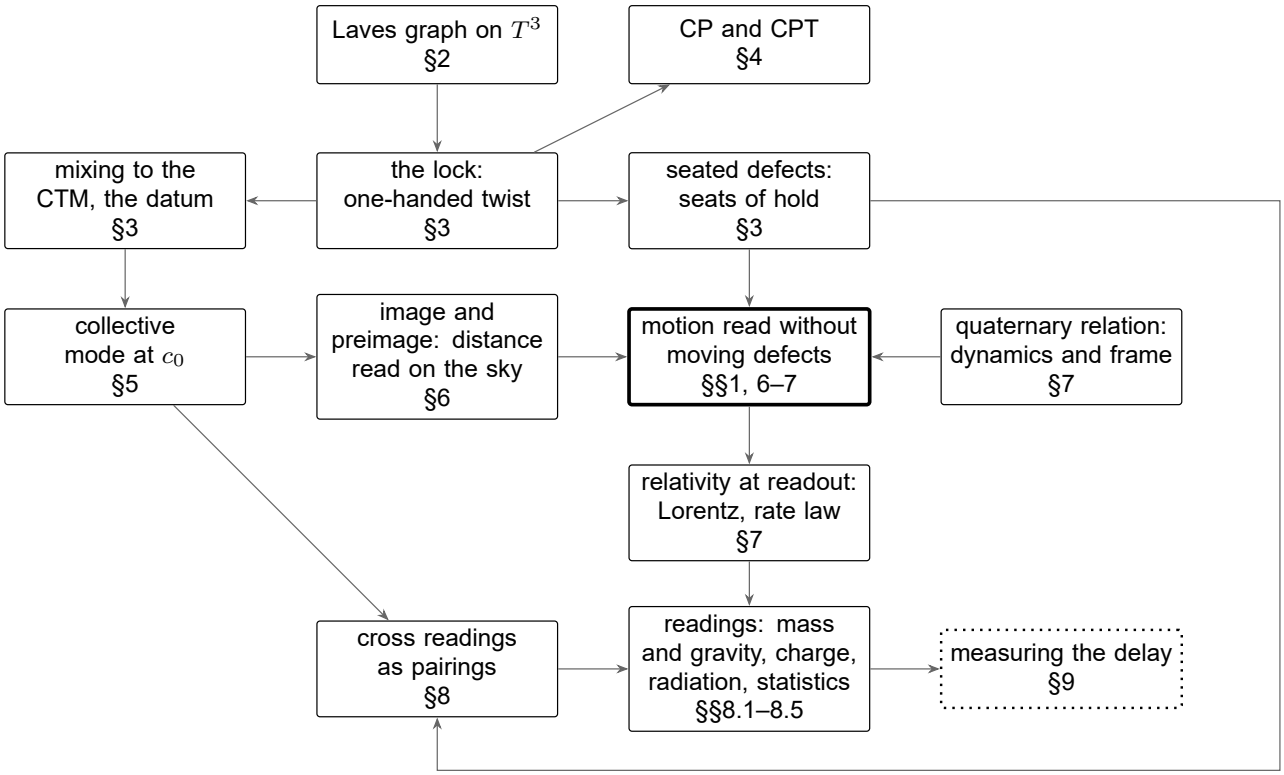

Figure 1: Claim dependencies; an arrow runs from a claim to one resting on it; each box names a claim and the section that states it; dotted: the open item of Section 9.

which alone a reader tells readings apart. The epistemic principles, premises that the theory takes and cannot prove from within, give the network its form (Appendix A): it stores no coordinate, no shared clock and no field; each edge is a band, a ribbon with two sides, and before the lock every update is reversible. **[F]** Criteria read from them select the Laves graph on the three-torus. **[R+I+M]** The lock writes a half twist of one handedness on every band and one more on the three bands of some vertices; at these overtwisted vertices, the defects, routes turn the other way, and only there can a pair of bits be held and released (Section 3). **[F+M]** Which vertices are overtwisted is primordial data, and no law below assumes a particular pattern. **[S]** A release forgets its pair's entry band, so a held state has several pasts and these merges write the arrow; routes then run in three helix families along the cube axes, and the network is a routing machine whose rules have no tunable parameter. **[F+M]** The lock mixes its flow into the causally trivial medium (CTM): statistically a uniform product state at composition $1/2$, an infinite-temperature state, which carries no signal of its own. **[R+M]** Of the symmetries that survive the lock (Section 4), the one read as CP stays exact with holds, given the declared reading of P. **[R+S+M]** The CP-odd data are therefore the handedness, which the lock reads, and the defect pattern. **[R]** CPT stays in the causal order, exact without holds and in distribution with them. **[R+S+F+M]** On the defect-free CTM route charges are conserved route by route and do not propagate, and one collective mode runs at $c_0 = v_{\text{bit}}/\sqrt{3}$, with v_{bit} the bit stride, in cells per tick (Section 5). **[F+M]** The readout part is physics under the relativity principle, taken apart into a quaternary relation (Section 7): dynamics is the relation of a reading's present window to a past one, and a frame is the relation of a source's windows to a reader's, each counted in its owner's ordinal, never in network ticks. Through declared conventions of rulers, clocks, light's speed as the conversion ratio between space and time, and statistics, the incidence transform turns this causal preimage into an image on the reader's sky (Sections 6 and 7); it decouples distance as well: a distance read is a property of the image, set by delays and directions on the sky, not the causal distance of the preimage on the network. **[R]** Motion is then a change of the image between windows, not a displacement on the network: no rule has to move a defect through the medium, and no reading meets the medium's

frame, the two problems met where particles are patterns moving over a substrate (cf. [1, 2, 3]). **[R]** Section 8 takes the readings, each with its grade.

2 The causal network on T^3 and its symmetries

Appendix A derives this network from the epistemic principles.

Graph. The graph of the network is the Laves graph [4], closed into the three-torus T^3. **[R+I+M]** The Laves graph is also the srs net of reticular chemistry [5], Wells' (10,3)-a [6] and Sunada's K_4 crystal [7]. **[F]** Every vertex meets three edges; the vertices fall into two classes, A and B, and each edge joins A to B; the shortest cycle has ten edges. **[F]** The quotient of the Laves graph by its translations is the complete graph K_4, with first Betti number 3, and the translations form a lattice of rank 3. The same construction on the honeycomb gives the theta graph, with first Betti number 2. **[F]**

Bands and registers. Each edge is a band with two sides. Each vertex carries a cyclic order of its three bands, the rotation system; numbered in this order, a band has the same number at both ends, so the bands fall into three band families, coloured in Fig. 2b. **[F]** Bits sit in entry registers, two at each end of a band, one on each side. Before the lock, the two sides of a band are its two strands, a route's two directions of motion (Section 5). The strand label $\chi = s \oplus [u \in \mathrm{B}]$, with s and u the side and vertex of the entry register holding the bit, $[u \in \mathrm{B}]$ the class bit and $\oplus$ exclusive or, names the two strands χ_1 and χ_0. One side carries only 1s and the other only 0s. A register and its mirror partner, the register on the other side at the same vertex (Fig. 3a), therefore hold exactly one 1 between them, and every band has occupancy $\rho = 1/2$, the fraction of registers holding 1. **[F]**

Ticks. Updates are counted by the network tick n, a local causal ordinal, not a global clock; before the lock their schedule is a gauge. **[F]** On 3- and 4-cell tori with random content, 12 of 12 asynchronous schedules agree with the synchronous run bit for bit. **[M]**

Routes before the lock. The path a bit follows when no event intervenes is its route. The turn at a vertex follows the side a bit arrives on, and before the lock a bit keeps its side. A route therefore turns the same way at every vertex and circles a face, the boundary walk the rotation system fixes. **[F]** These face loops are open three-step helices about the four body diagonals $\langle 111 \rangle$ (Fig. 2g), one family per diagonal, and together they span a lattice of rank 3 (Appendix B). **[M]**

Symmetries and conventions. Before the lock the flow's exact symmetries are the translations and five operations. The body-centre translation t_{bc} exchanges the classes and keeps every side. The fourfold screw rotation Rot_4 is a proper rotation; it permutes the band families oddly and flips the strand. The complement X exchanges 0 and 1 in every register. Causal reversal J_{hist} is the inverse of the update. State reversal J_{state}, Wigner's motion reversal, sends each register across the band its bit leaves by, at its vertex, and keeps the class; the same rules then run forward, and side 1 is side 0 run backwards. **[F+M]** Before the lock every update is a bijection, and with the time-reversal symmetry J_{state} the flow has no readable arrow. **[F+M]** Four labels are conventions: the direction of circulation, the choice of rotation system, which class is named A, and which side is called 1. **[S]**

3 The lock and the routing machine

The lock. The lock writes on every band a half twist of one handedness, $\Upsilon = \pm 1$, chosen before the lock. A bit now changes side on every band, so its turns alternate and its route runs straight (Fig. 3a, b). Each route uses two of three band families, so routes form three helix families, one along each cube axis (Fig. 2e, f), and no fourth. **[F+M]**

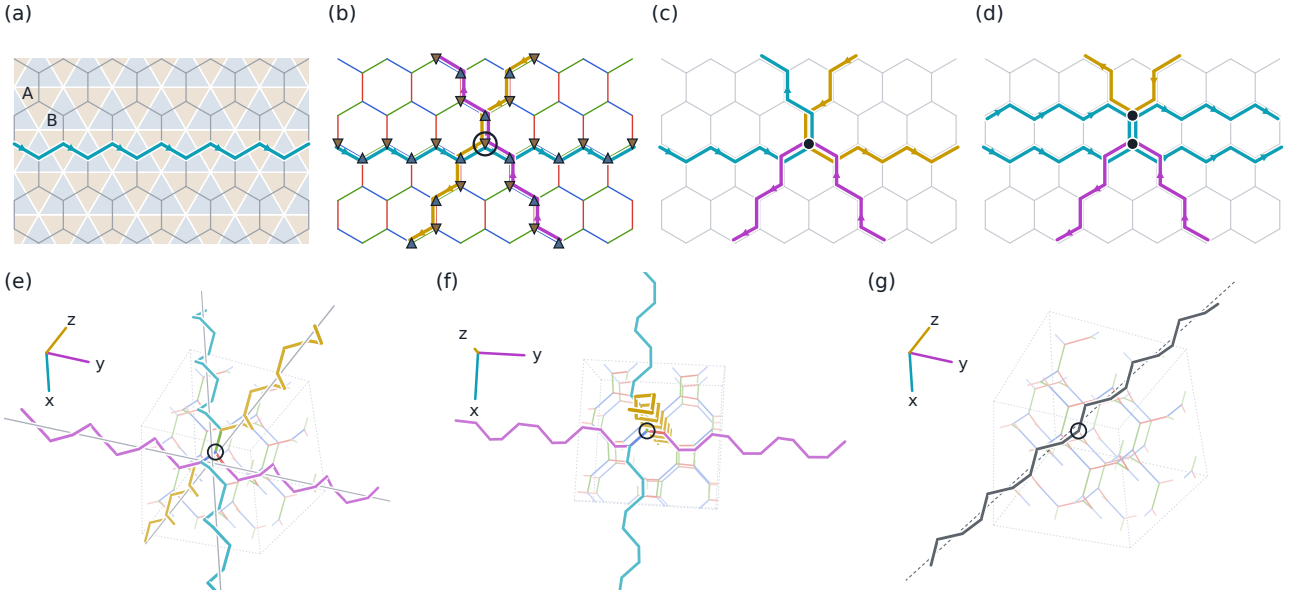

Figure 2: Routes under the rule of the Laves graph, on the honeycomb, (a)–(d), in the plane only for readability, and on the Laves graph, (e)–(g). A ring marks the vertex the routes pass through, a black dot an overtwisted vertex. (a) Vertices at the centres of dual triangles, A down (warm grey), B up (cool grey). (b) Bands coloured by band family (red, green, blue), triangles marking the classes as in (a); each route takes the additive mix of the two families it alternates between. (c) An overtwisted vertex. (d) An adjacent overtwisted A–B pair. (e) Routes along the cube axes, coloured as the axis marker; grey lines, the helix axes. (f) The view of (e) about 6° off one axis. (a)–(f) are routes after the lock; (g) is one before it, in the view of (e): a face loop advancing one body-centring vector per period along a body diagonal (dashed).

Overtwisted vertices. At an overtwisted vertex each band carries one more half twist of the lock's handedness, so the number τ_e of half twists on band e is 1, 2 or 3 as none, one or both of its ends are overtwisted (Fig. 3c). **[F+M]** A bit arriving there reaches the other register and turns the other way: its route turns a third of a turn into another helix family (Fig. 2c), or, through two adjacent overtwisted vertices, turns twice in opposite senses and shifts by one row (Fig. 2d). **[F+M]** Overtwisted vertices are the only seats of hold, where a pair can be held and released. **[F]** No rule moves them: the routing moves content, and the lock's twists stay written in the bands. **[F]** Their pattern is primordial data, and no law below assumes a particular pattern. **[S]** Whatever the lock's rule, the pattern is discrete with finite mean density. **[F]** It is taken statistically uniform above some scale and aperiodic, unlike the pattern with every A vertex overtwisted. **[S]** As an ensemble it is balanced over the four orientations of the threefold axes, lest its rest frame be preferred. **[R+M]** Motion needs no such move (Section 1), so Minimal sufficiency (Appendix A.1) leaves out a rule that cuts and reglues bands. **[R]** Rates and readings do depend on it: a drifting causal flow's loss of lattice momentum on their density, and the held content of two closures (closed routes through overtwisted vertices), each with seven overtwisted vertices, by about 1.9% of an isolated overtwisted vertex's held content (Section 5). **[M]**

Swap and hold. Only a twisted band hosts a swap, the exchange that lets a pair of bits cross it as if untwisted, so before the lock none fires, though pairs of equal bits do meet, the lock having written no twisted band. **[F]** The twisted region is thus a new phase. Any half twist makes a band a venue; counting only odd numbers of half twists would bar swaps on bands with one overtwisted end. **[S]** The routing machine has two events. A swap fires in the only two occupancies of a twisted band where crossing as if untwisted changes the outcome but no strand count; no record shows which bit continued which. **[F]** On the CTM swaps fire at $1/8$ per band per tick (measured 0.1248 ± 0.0002), the clock. **[F+M]** A hold captures a pair at a seat and releases it on its entry band, delayed, or on another

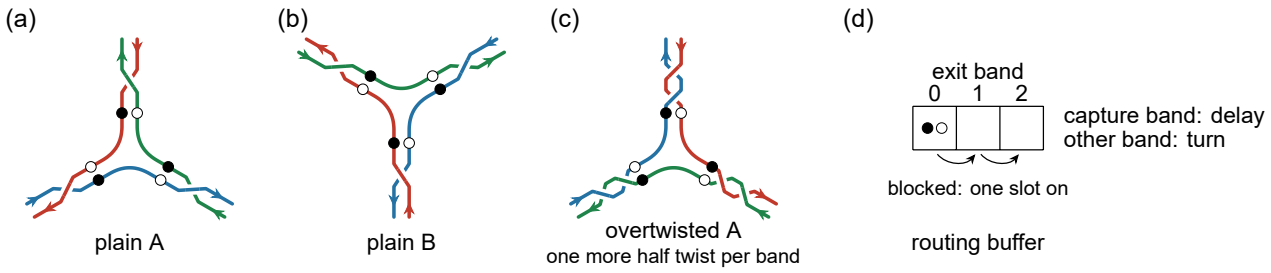

Figure 3: Bands at a vertex. Each stub is half a band; its two sides cross once at the band's midpoint, the lock's half twist. Each side carries χ_1 along its arrow and χ_0 against it; filled and open dots are the χ_1 and χ_0 entry registers. (a) Plain A vertex: χ_1 turns right. (b) Plain B vertex: χ_1 reversed, turns left. (c) Overtwisted A vertex, one more half twist per band: χ_1 reaches the open dot and turns left, one exchange of strands relative to (a). (d) A seat's routing buffer, indexed by the held pair's exit band.

band, turned (Fig. 3d). **[S]** Both classes share one release table. **[M]** Routing reads a single bit per band. The strand label of Section 2 is constant along a route, and each tick conserves both strand counts. No rule has a tunable parameter. **[F]**

The tick. A tick updates every vertex at once (Appendix C): a seat releases its held pair once both registers of the exit band are empty, and an empty seat captures a pair arriving on mirror registers; then the swaps fire, and every free bit moves on along its route. **[S]** The order within a tick, swap detection before routing, is a choice (Appendix C). **[S]** With holds and swaps on, 48 more asynchronous schedules agree (Appendix C.2). **[M]**

The arrow. A release forgets its pair's entry band, so a held state has several pasts: J_{hist} does not exist at a seat (Appendix B.6), and these merges write the arrow, before the whole finite system reaches its Poincaré recurrence. **[F+M]** The handedness is not broken but read: Υ is chosen before the lock, and routing reads it only through its product with a vertex's class; Inv reflects the embedding and with it handedness and turning sense together, leaving the turn the rules produce unchanged. **[F+M]**

Mixing into the CTM. Given the twisted band as venue, the twist must be written while content crosses the band; twists written between ticks never mix. **[F]** The lock also mixes the flow: its twist is written by a front that crosses the network, content is unprotected at each band's first twisted crossing, and a twist written everywhere at once, with no overtwisted vertex, would not mix. **[F+M]** Behind the front, content at a band is mixed within a few ticks of the twist's arrival, and each side's composition settles at $1/2$. **[M]** This is the causally trivial medium (CTM), a state of the flow, not stored structure; no rule refers to it. **[F]** Averaged over 64 seats, the joint probabilities of j registers lie within 1.1% of 2^{-j}; seat by seat they deviate by 13–21%, several times the sampling scatter for $j \leq 4$, read as a static imprint of the seat's own structure (Section 7). **[I+M]** Statistically a uniform product state, it carries no signal of its own: a reader on it reads the reference, up to noise. **[R+M]**

4 Discrete symmetries after the lock

The lock leaves three tiers of discrete symmetry: operations exact with holds, operations exact only on the defect-free CTM, and a static invariant of the bands. Section 7 assigns the read-as names.

Exact with holds. The operation Mir keeps every position and every half twist and reverses the rotation system at every vertex. The twofold rotation Rot_2 about a face diagonal permutes the band families oddly, as Rot_4 does. **[F]** The inversion Inv reflects every position through a point, and with it the band embedding, the twists the lock writes; the diagonal mirror is $\sigma_d = \mathrm{Inv} \circ \mathrm{Rot}_2$. Each of t_{bc}, Rot_4, Rot_2 and Mir reverses the turning of every hold; a product of an even number of them restores every hold, and one or three do not. **[M]** Hence $t_{\mathrm{bc}} \circ \mathrm{Rot}_4$, $t_{\mathrm{bc}} \circ \mathrm{Rot}_2$, $\mathrm{Mir} \circ \mathrm{Rot}_4$ and $\mathrm{Mir} \circ t_{\mathrm{bc}}$ are exact bit by bit with holds, as are the primitive translations, the threefold rotation about a body diagonal and the twofold rotation about a cube axis. **[M]** X exchanges 0 and 1 while holds capture only 1s. **[S]** At the seats t_{bc}, Rot_4, Rot_2, Mir and X each break alone, as do the four products with X that were run and $\mathrm{Mir} \circ t_{\mathrm{bc}} \circ \mathrm{Rot}_4$. On tori of 4 and 6 cells at defect densities up to 0.2 and 0.1, two seeds and 300 ticks each, every exact operation matches on every tick and every broken one fails on every tick from the first; fixed test patterns, chosen placements of overtwisted vertices, on tori of 8 and 12 cells give the same. **[M]** For every proper isometry g exactly one of g and $\mathrm{Mir} \circ g$ is exact with holds: $\mathrm{Mir} \circ g$ if and only if g either exchanges the classes or permutes the cube axes oddly, but not both. **[M]** Fourfold rotations and twofold rotations about face diagonals are odd, the rest even. **[F]** On a 12-cell torus the 82 944 such operations form 48 cosets of the exact, class-keeping primitive translations and 23 geometric classes; one operation of every coset and three of every class, each tested in both forms, g and $\mathrm{Mir} \circ g$, over 300 ticks with holds on a fixed pattern of overtwisted vertices, obey the law. **[M]** It extends the parity of the turning above to every proper isometry, screws and translations included. **[F+M]** With no overtwisted vertex, both forms are exact, so Mir is seen only through overtwisted vertices; with them, all four combinations of class exchange and Mir occur among the exact operations. **[M]** The exact $t_{\mathrm{bc}} \circ \mathrm{Rot}_4$ flips every side, keeps every strand and maps the state before the lock (Section 2) to its complement, so which side is called 1 is carried by an exact symmetry. **[F+M]** It stays exact while the lock's front crosses the network. **[F+M]** (Check D16.)

One orbit of handedness and class. The handedness Υ and the class of the seed, the vertex where the lock's front starts, give four labels on one orbit (Fig. 4a). The product $t_{\mathrm{bc}} \circ \mathrm{Rot}_4$ exchanges the classes at fixed handedness. The product $t_{\mathrm{bc}} \circ \sigma_d$ exchanges the classes and reverses the handedness, and is exact with holds. The mirror σ_d alone reverses the handedness at fixed class and breaks at holds, since it flips the strand; the inversion Inv changes no machine label, so on the machine σ_d acts as Rot_2 and $t_{\mathrm{bc}} \circ \sigma_d$ as $t_{\mathrm{bc}} \circ \mathrm{Rot}_2$. The lock is therefore written alike from either seed class at either handedness. **[F+M]** The operations Mir and σ_d are distinct (Fig. 4a, b): the first reverses only the rotation system, keeping the handedness; the second reflects the positions and so the handedness. **[F]**

Exact on the defect-free CTM only. On the defect-free CTM, where the singles above are exact too, three more operations are exact bit by bit: the complement X, the state reversal J_{state} and their product $X \circ J_{\mathrm{state}}$, checked on tori of 8 and 16 cells at $\rho = 1/2$, and for J_{state} also at $\rho = 0.3$, off the CTM's composition, over 30 ticks. **[M]** This paper takes the state reversal (Section 2) to pair the two strands on a band, reading the strand χ_0 as χ_1 run backwards. **[S]** With holds on, J_{state} still matches the forward run in distribution: on a 12-cell torus over six seeds the occupancy per overtwisted vertex differs by -0.0004 ± 0.0004. **[M]** So does $t_{\mathrm{bc}} \circ \sigma_d \circ J_{\mathrm{state}}$, whose run is the $t_{\mathrm{bc}} \circ \sigma_d$ image of the J_{state} run on every seed. **[F+M]** Causal reversal J_{hist}, the inverse of the update, does not exist at a seat (Section 3), and that alone makes these reversals fail trajectory by trajectory: the arrow is written in the rules, not in a boundary condition, and the reversal available to the readings is J_{state}. **[F]**

A static invariant. Each band carries a framing $\tau_e/2$, set by its half twists in the band embedding and readable at the band, which no event after the lock changes. The framing is t_{bc}-even and J_{state}-even, and even under reflection when counted relative to the lock's handedness. **[F+M]** Routing and holds do not read it, except on the bands of an overtwisted vertex, which carry two half twists: there a quantum of framing of the opposite handedness would leave none and close the venue. One reading sees it everywhere: a sum over walks along routes that weights each move out of an overtwisted vertex by

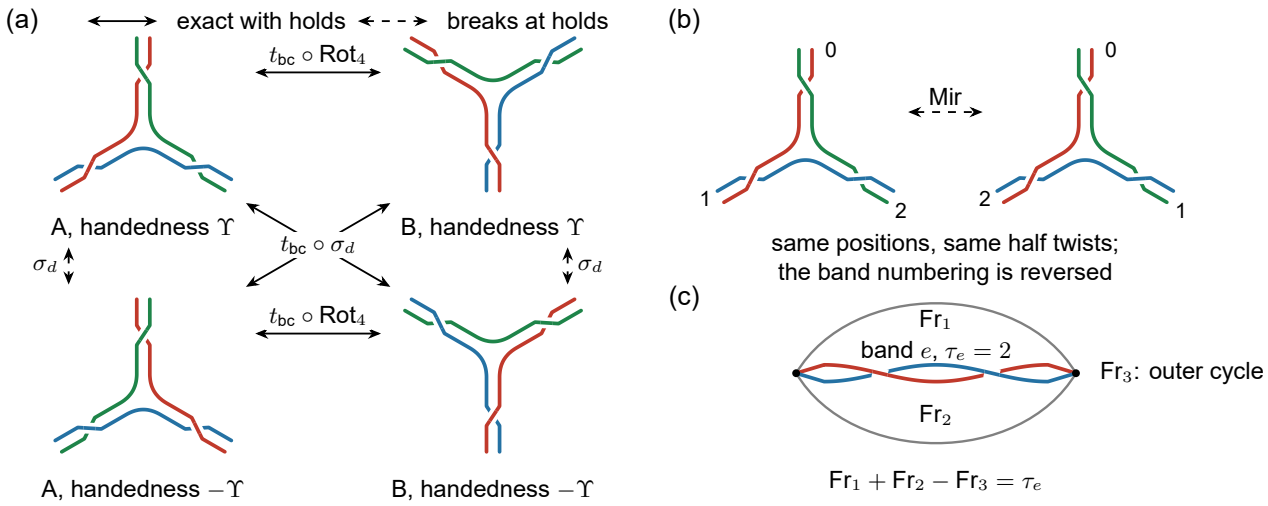

Figure 4: Handedness, class and framing. The icons are the bands of Fig. 3a, b without arrows or registers. (a) The four labels on one orbit; the lower row is the mirror image of the upper. (b) Mir reverses the band numbering at fixed positions and half twists. Solid arrows: exact with holds; dashed: breaks at holds. (c) One band e with two half twists in a theta graph; Fr_1 and Fr_2 are the framings of the two cycles that share only e, and Fr_3 that of the outer cycle.

the phase factor $\exp(i\lambda\theta)$, with $\theta = \pm 2\pi/3$ the turn signed by the side of the band and λ the phase weight, reads at $\lambda = 1/2$ the sign -1 raised to the total framing around a loop, counted relative to the lock, an Aharonov–Bohm-type sign, one $\mathbb{Z}_2$ flux per loop (Section 5). **[F]** A quantum of framing cannot hop to a neighbouring band unseen: on a 3-cell torus all 1296 such moves, checked exhaustively, change the signs this reading sees. The smallest event that changes a framing is a pinch, the two sides of one band passing through each other, which changes the band embedding. **[F+M]** Fig. 4c shows one band's framing read on a theta graph; Appendix B gives the integer and sign layers.

Sign ledger. Table 1, the sign ledger, lists the labels each operation keeps or reverses. Its label entries hold on all 384 registers of a 2-cell torus. **[M]** Its last column comes from the runs above. **[M]** The column w is the closure index, the turning number of a closure, a closed route through overtwisted vertices; the overtwisted A and B vertices of a closure differ in number by $3w$. **[F]** The band-rotation sign h is the sign of a route's band rotation per turn; every proper operation keeps it, and Inv, σ_d and $t_{bc} \circ \sigma_d$ reverse it. **[F]** The route-charge sign q is the sign of the turn a release gives a route; it is reversed by t_{bc} and kept by Rot_2 and J_{state}. It is therefore kept by Rot_4, which acts on every machine label as Rot_2 does, and by σ_d, since Inv changes no machine label. **[F]**

The forced consequence. The exact $t_{bc} \circ Rot_4$ sends (q, h) to $(-q, h)$, so the machine's laws give, over any ensemble that weights each pattern of overtwisted vertices like its image, the law-level zero

$$\langle q \cdot h \rangle = 0. \tag{1}$$

A pattern of overtwisted vertices may correlate q with h, but its image under $t_{bc} \circ Rot_4$, run by the same rules, carries the opposite correlation. **[F+M]** Reading a correlation of q with h, as the weak interaction's chirality, belongs to the readout layer and is left open (Section 9). **[R]** A related limit binds the lock: a lock rule that reads only the handedness cannot write a t_{bc}-odd integer, because t_{bc} is a translation and keeps the handedness. **[F]** Whether such a rule must read the product of handedness and class at a vertex is untested.

Operation	class	χ	band order	Υ	h	w	bit value	with holds
t_{bc}	swap	$-$	$+$	$+$	$+$	$-$	$+$	breaks
Rot_4, Rot_2	$+$	$-$	$-$	$+$	$+$	$+$	$+$	breaks
Mir	$+$	$-$	$-$	$+$	$+$	$+$	$+$	breaks
X	$+$	$+$	$+$	$+$	$+$	$+$	$-$	breaks
J_{state}	$+$	$-$	$+$	$+$	$+$	$+$	$+$	in distribution
Inv	$+$	$+$	$+$	$-$	$-$	$+$	$+$	invisible
σ_d	$+^{\dagger}$	$-$	$-^{\dagger}$	$-$	$-$	$+$	$+$	breaks
$t_{\mathrm{bc}} \circ \mathrm{Rot}_4$	swap	$+$	$-$	$+$	$+$	$-$	$+$	exact
Mir $\circ\, \mathrm{Rot}_4$	$+$	$+$	$+$	$+$	$+$	$+$	$+$	exact
$t_{\mathrm{bc}} \circ \sigma_d$	swap†	$+$	$-^{\dagger}$	$-$	$-$	$-$	$+$	exact
$t_{\mathrm{bc}} \circ \sigma_d \circ J_{\mathrm{state}}$	swap†	$-$	$-^{\dagger}$	$-$	$-$	$-$	$+$	in distribution

Table 1: Sign ledger. Entries: $+$ kept, $-$ reversed, swap for A and B exchanged; a dagger marks an entry composed from the rows of the factors. Band order is the cyclic order of the bands at a vertex; Υ is the geometric handedness. Every operation is exact on the defect-free CTM, where J_{state} and the last row are reversals ($S \circ \mathcal{U} \circ S^{-1} = \mathcal{U}^{-1}$, S the operation, $\mathcal{U}$ the update) and the others commute with $\mathcal{U}$, carrying the pattern of overtwisted vertices along; the last column says whether it stays exact with holds on, "invisible" meaning that it changes no machine label: the Laves graph is chiral, so Inv maps the net to its mirror image. The route-charge sign q transforms as w on every row. **[F+M]**

5 Coarse-graining and its fixed points

Coarse-graining the CTM of Section 3 keeps only its conserved densities, and their behaviour under the operations of Section 4 sets their transport.

Densities and route charges. The number density N counts $\chi_1+\chi_0$, with N_a its part on routes along cube axis a; the strand-difference density Q counts $\chi_1-\chi_0$; the route charge Q_R is the strand difference along a route R. A swap reflects Q and transmits N; on the one-dimensional skeleton of a route family, Q is then carried by a permutation that N fixes, linearly and without self-interaction. **[F]** On each route the strand is the direction of motion, χ_1 forward and χ_0 backward, so Q_R is the net flow along R. With p the density of overtwisted vertices, every route conserves its Q_R exactly at $p = 0$. A hold changes Q_R only when its entering pair spans two routes, and at an isolated overtwisted vertex all three corners lie on one route. **[F]** Machine runs conserve every Q_R, with holds off and on (Appendix D.2). **[F+M]** The difference between the registers of the two classes, signed alternately by tick, gives a second set of route charges K_R, also conserved route by route at $p = 0$ (Appendix D.2). **[M]** Both route charges are t_{bc}-odd. **[F]**

Lattice momentum and the collective mode. The lattice momentum $\mathcal{P}_a$ along cube axis a is the sum of $v_{\mathrm{bit}} Q_R$ over the routes along a, each signed by its orientation, with v_{bit} the bit stride, a route's stride along its cube axis, one cell per four-tick helix turn (along a bond a bit moves 0.35 cell per tick). It is t_{bc}-even and conserved route by route. Along each route family the number and the strand difference are each other's current, so the lattice momentum flux is

$$\Pi_{aa'} = \delta_{aa'}\, v_{\mathrm{bit}}^2 N_a, \tag{2}$$

diagonal, with no shear stress. Linear flow under this flux has one collective mode, the sound mode of lattice gases [8, 9], with stride

$$c_0 = v_{\mathrm{bit}}/\sqrt{3}, \tag{3}$$

independent of ρ. **[F+M]** Its isotropy follows from the three orthogonal route families, the exact flux (2) and equal family weights at rest: given local equilibrium about the stationary measure of a drift (Appendix E), in which routes along $+a$ have occupancy ρ_a at $\rho = 1/2$, the collective mode along the unit

wavevector $\hat{k}$ has

$$c^2(\hat{k}) = v_{\text{bit}}^2 \frac{\sum_a \hat{k}_a^2 \rho_a(1-\rho_a)}{\sum_b \rho_b(1-\rho_b)}. \tag{4}$$

At rest every ρ_a is $1/2$, so $c_0 = v_{\text{bit}}/\sqrt{3}$ in every direction. **[F]** A cube-axis drift makes the weights $\rho_a(1-\rho_a)$ unequal; a drift along $\langle 111 \rangle$ leaves them equal and shifts the stride at no order. **[F]** With $v_{\text{bit}} = 0.25$ cell per tick, $c_0 = 0.1443$ cell per tick; the machine gives c_0 to 0.1% and the second-order anisotropy below (Appendix D.2). **[M]** A drifting causal flow carries a uniform lattice momentum, and its drift is that flow's stride. The CTM symmetry $X \circ J_{\text{state}}$ sends $(\rho, \mathcal{P})$ to $(1-\rho, \mathcal{P})$ and reverses the updates, so at $\rho = 1/2$ a drifting causal flow has no first-order splitting of the collective-mode strides along and against the drift. **[I]** At second order the drift makes the collective-mode stride anisotropic with the lattice, slower along a cube-axis drift and faster across it, as Eq. (4) gives (Appendix E). **[F]**

Densities odd under t_{bc} do not propagate. By the selection rule of t_{bc}, densities odd under it decouple from propagation at linear order. Both route charges are odd and conserved route by route, so they can only freeze or diffuse, while N and the longitudinal lattice momentum carry the collective mode. **[F+M]** Only N peaks at $c_0 k$ in the machine's spectra (Fig. 8, Appendix D.2). **[M]**

Overtwisted vertices as sinks. A Darcy sink loses lattice momentum at a rate proportional to it, so the momentum decays exponentially. Overtwisted vertices drain lattice momentum although every route charge survives: an overtwisted vertex merges routes of different directions, and diffusion along the routes then spreads Q_R over them. **[F+M]** At short times they act as Darcy sinks, but the measured decay has a power-law tail in $p\sqrt{n}$, not an exponential (Appendix D.2). **[M]**

Two theorems. An object is a test body, a closure that a run moves between ticks, outside the rules; the rules never move an overtwisted vertex (Section 3). Drag is the mean lattice momentum that the CTM takes up per tick from a moving object.

Theorem 1 (zero drag)**.** *On the CTM itself, with the uniform product measure at $\rho = 1/2$, any reversible, number-conserving dynamics of an object without holds has mean drag exactly zero at any stride.*

With fixed routing each tick is a number-conserving bijection, and changing the routing moves no content. Any history is therefore a composition of such bijections, each preserves the uniform product measure of the CTM, and the expected change of $\mathcal{P}$ vanishes. **[F]** On the machine, which realises that measure only approximately, a 14-vertex closure and holds that only delay drag within one standard error of zero, an irreversible release does not (Appendix D.2). **[M]** On the CTM itself, drag therefore comes only from irreversible coupling. **[F+M]**

Theorem 2 (routing modulation)**.** *On the CTM itself, with the uniform product measure at $\rho = 1/2$, any reversible, number-conserving variation of the routing at overtwisted vertices writes no phase-locked line, a sharp peak at its frequency, in the spectrum of the mean occupancy; every one-time average stays constant.*

Without holds each tick is a routing permutation composed with a swap on each band, a bijection that conserves number and both strands, and it preserves that measure. **[F+M]** Theorem 2 is the frequency form of Theorem 1: a phase-locked line can be written only by holds. **[F]** On a fixed test unit the machine writes a phase-locked line with holds and none without (Appendix D.2). **[M]**

Static readings. In the walk model a reading is a walk sum $\mathcal{G}_\lambda$ over killed walks along routes, which end at each step with a small probability, weighting each move out of an overtwisted vertex by $\exp(i\lambda\theta)$ (Section 4; for charge, θ signed by vertex class). At $\lambda = 0$, $\mathcal{G}_0$ is exactly additive for any doubly stochastic routing, with stationary weights fixed by the hold fraction at each vertex (Appendix E). It is therefore independent of shape, of routing, of closure length and of the closure index w. **[F]** In the walk

model the reading is additive up to a small deficit (Appendix D.2). **[M]** Every reading is a killed-walk resolvent whose step matrix is bounded entrywise by a doubly stochastic one, and the killing puts its spectral radius strictly below 1 for every routing, rule, λ, handedness and twist. The readout map, the resolvent as a map from the torus of boundary angles, one per cycle of T^3, into the invertible matrices, is therefore null-homotopic for every routing and phase factor: its determinant winding and its three-dimensional winding number vanish. **[F]** In the walk model the winding number tends to zero with the grid (Appendix D.2). **[M]** A unit is a cluster of overtwisted vertices, and a trail is a chain of overtwisted vertices along a path, with two ends. For a unit built from trails, a local probe even under t_{bc} sees only the trail ends: each trail reads its end sign times a combination of its end and inner responses, independent of its length up to a small finite-length correction measured on a fixed test pattern (Appendix D.2), and the balance of signs over the two classes cancels any response affine in the vertex degree. **[F+M]**

Fixed points. Under the hydrodynamic hypothesis that after coarse-graining only real-valued conserved densities with Gaussian fluctuations remain, the space of order parameters, the values these densities can take, is contractible, with vanishing second and third homotopy groups; with route charges conserved route by route, the stationary state may instead be a generalized Gibbs ensemble. **[I]** At $p = 0$ the collective mode propagates with dynamic exponent 1, its stride isotropic within 1% down to wavelengths of 7 cells, a damped sound mode (Appendix D.2). **[M]** The transmission-line model (Appendix C) is the lossless low-k limit of this mode. **[I+M]** At $p > 0$ the sinks also attenuate the mode, and Γ grows superlinearly in p above $p = 0.1$ (Appendix D.2). **[M]** The mode's diffusive limit, exponent 2, is not observed (Appendix D.2). **[I]** The integers left to the readings are $\mathbb{Z}_2$ statements and index laws, such as the law that ties w to the overtwisted vertices of a closure. **[I]** This paper takes the turning phase of the $\lambda = 1/2$ channel (Table 2) in its $\mathbb{Z}_2$ form, flat on the CTM; the channel is then gapless there. **[I+S]** Each overtwisted vertex carries one π flux: on a 32-cell torus the transitions of sign -1 in that channel are exactly the three from each of the six registers of each overtwisted vertex. The fluxes sit on vertices, so the phase factor is $\mathbb{Z}_2$ only and winds around no line. **[F+M]** A closure contains one flux per overtwisted vertex, and their number has the parity of w, since the A and B counts differ by $3w$. **[F]** With overtwisted vertices at density p the π fluxes screen the $\lambda = 1/2$ channel: in the transmission-line model with these fluxes the static response to a point source falls off over $\ell = (D_{\mathrm{tl}}/\Delta)^{1/2}$, with Δ the static operator's gap, its lowest eigenvalue, and D_{tl} its stiffness at $p = 0$, and $\ell \propto p^{-0.54}$ (Appendix D.2). **[M]** This is the form of independent static absorbers, $\ell^{-2} \propto p\,(1 - \cos\Phi)$ for a phase Φ per overtwisted vertex: the class-signed phases $\pm\pi/3$ of the charge rule screen too (Appendix D.2). **[I+M]** At $\lambda = 0$ every phase factor is 1, so the operator is the one at $p = 0$: no screening (Appendix D.2). **[F+M]** With lossy overtwisted vertices the $\lambda = 0$ excitation instead takes a gap from their unsigned density (Section 8.3). **[M]** The pattern screens coherence, second order in Φ, of a single content's $\lambda = 1/2$ propagation; the charge reading is first order, carried by the $\lambda = 0$ kernel, and not screened (Section 8). **[F]** (Checks D7, D17, D18.)

Identity. By the additivity of $\mathcal{G}_0$, units with equal held content are identical in what $\lambda = 0$ reads. **[F]** The held content of a unit, averaged over ticks, is that of its overtwisted vertices taken one by one, less $0.96\% \pm 0.06\%$ of one isolated overtwisted vertex for each adjacent A–B pair; it does not depend on w, on closure length or on any further arrangement (Appendix D.2). **[M]** Closures of 14 and 18 vertices differ in held content and are not identical (Appendix D.2). **[M]**

6 The incidence transform

A reader's sky is a sphere S^2 of directions, and coarse-grained at the reader the arrival frames over it, each a direction and a fibre angle about it, form the Hopf fibration over the sky, absent on the network. **[Cand]** The incidence transform is the reader's demodulator, the inverse of modulation, turning arrivals into readings on this sky; space, time and motion, the words of the readout space, enter the

paper here as its candidate readings.

The signal chain. The medium is the CTM, which carries no signal of its own (Section 3). **[R+M]** If its space of order parameters is contractible (Section 5), the CTM has no topological defects, by their homotopy classification. **[F]** Curvature in a reading then comes from the transform. **[Cand]** The carrier is the $\lambda = 0$ collective mode at c_0 (Section 5), whose stride the readout layer reads as the speed of light. **[R]** Overtwisted vertices, and the sources built from them, modulate the flow: a hold delays it, and a release turns it (Section 3). **[S]** A reader, a seated closure, counts arrivals in its own ordinal ν through a fixed window (Section 7). **[R+S]** Its demodulator pairs three data of an arrival with three conjugates (Table 2): the arrival tick with a frequency ω, whose group delay gives depth; the place across the reader with a wave vector, whose direction is a point of the sky; and the rotation of the arrival frame about that direction, its fibre angle, with the phase weight λ, which Section 7 reads as a spin weight. **[Cand]** On the network $\theta = \pm 2\pi/3$ is a route's change of direction at a vertex, not the fibre angle; λ weights the turns at overtwisted vertices (Section 5), so λ counts only modulo 3, and $\lambda = 1/2$ only through the double cover. **[F]** At the reader λ is a harmonic of the continuous fibre angle. **[R]**

Reader: flow lines and the sky. A flow line is a route followed into a reader. The sky $\mathcal{S}_o$ of a reader o is the sphere of directions $\hat{n}$ of the flow lines through o, coarse-grained at o (Fig. 5a). Each arrival carries an arrival frame, its direction on the sky and a fibre angle about it, which the half twist of every band, of framing $\tau_e/2$, covers twice (Section 4; Table 3, D6). **[R]** Against parallel transport a route's band rotates by the tetrahedral angle $\arccos(-1/3) = 109.47^\circ$ per step, four steps per helix turn (Fig. 2f), so by 437.88° per turn; with the path's Berry angle, -77.88°, it makes exactly one turn, with the band-rotation sign h of Section 4, as the Călugăreanu–White–Fuller theorem requires [10, 11, 12]. **[F+M]** With the Berry angle, a flow line's fibre angle depends only on its end frames: it takes four values, only 0 of them on the 120° lattice, and is continuous once coarse-grained onto the sky direction. **[S+M]** A beamformer, a reader of several units that weights their arrivals by a plane wave's phase gradient along $\hat{k}$, reads that direction, and its beam width, which follows the Fourier law of the aperture, is the sky's resolution cell. **[R]** A reader of one vertex, reading the mean of its edges, resolves no direction, by construction. **[F]** In a pilot in the transmission-line model, with sources along $\langle 100 \rangle$, $\langle 110 \rangle$ and $\langle 111 \rangle$ at $\lambda = 0$ and $1/2$, the beam peaks 0.8–2.4° from the source in 18 of 18 cases, against quarter beam widths of 12–32°, and its width is within 15% of an ideal aperture in 6 of 6 cases; a one-vertex reader's three edges, phased as a small array, show a weak direction dependence, beyond an ideal three-point aperture in 3 of 14 cases. **[M]** (Checks D14, D20.)

Demodulator: a windowed transform. The window makes the transform a short-time Fourier transform. **[R]** For the demodulator's three pairs, under one fixed window sharpening one member of the first two blurs the other, while the third, fibre angle and λ, is a Fourier series on a circle: λ takes

Channel	Sensitive to	Read as	Grade
$\lambda = 0, \omega = 0$	counts, dwell, the $1/r$ static offset	rest mass the potential, as the static, $\lambda = 0$ part of a spin-2 reading, the declared choice giving $\gamma_{\text{PPN}} = 1$	**[R]** **[R+S]**
$\lambda = 1/2, \omega \to 0^+$	turning signs on the double cover	helicity h, with the closure sign $(-1)^w$ charge, from w, the Coulomb reading	**[R]** **[R+S]**
$\lambda = \pm 1, \omega \neq 0$	first harmonic of the fibre angle: frame relations of source and reader	light's two polarizations	**[R]**
$\lambda = \pm 2, \omega \neq 0$	second harmonic of the fibre angle; degree $\pm 4\Upsilon$, against $\mp 2\Upsilon$ at $\lambda = \mp 1$	gravitational radiation	**[R]**

Table 2: Channels by demodulation frequency ω and phase weight λ; checks by channel: D1, D4; D6, D9; D6; D14 (Table 3).

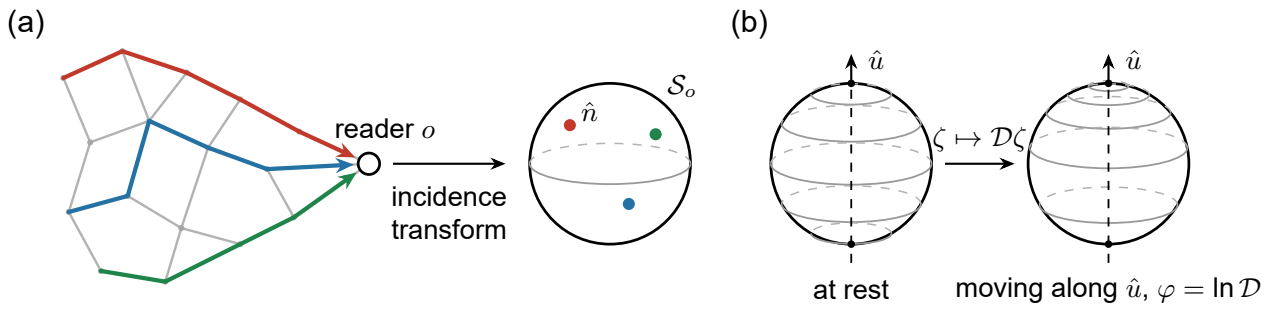

Figure 5: The reader's sky. (a) Routes, drawn as an abstract net, arrive at a reader o, and the incidence transform makes each arrival a point $\hat{n}$ of its sky $\mathcal{S}_o$. (b) Motion stretches the sky by the Doppler factor $\mathcal{D} > 1$ along $\hat{u}$: in the stereographic coordinate ζ, zero at the rear pole on the axis of motion $\hat{u}$, $\zeta \mapsto \mathcal{D}\zeta$; circles at fixed angle to $\hat{u}$ crowd towards the forward pole. Does not carry over: positions in the readout space and the lengths and angles of the drawn net; only arrivals carry over.

discrete values, which no window blurs. **[Cand]** A reading of weight λ is a section of a line bundle over the sky of degree $2\lambda\Upsilon$; a source enters only the section, so the signed zeros of a reading over the sky add up to $2\lambda\Upsilon$ whatever the source's closure index w, the index Section 8 reads as charge. **[R]** On the sky $\lambda = 2$ and $\lambda = -1$, equal on the network, have degrees 4Υ and -2Υ, and their magnitudes differ direction by direction (Table 3, D14). **[R+S+M]**

Motion on the sky. Motion acts on a sky by a Möbius map: in the stereographic coordinate ζ with poles on the axis of motion $\hat{u}$, the stretch $\zeta \mapsto \mathcal{D}\zeta$, with $\mathcal{D}$ the Doppler factor along $\hat{u}$ (Fig. 5b). Rotations of the sky are compact and cannot compose to a stretch, so the rapidity $\varphi = \ln \mathcal{D}$ read by counts out and back lives on the source–reader line. **[R]** Seated readers and sources do not move (Section 3). Between two of them the counts out and back stay bounded, so the two factors multiply to 1; their reciprocal part, equal out and back, is motion and is 1, and the relative velocity is zero (Picture 1; a picture box maps an everyday case onto the network and states what does not carry over). What can remain is anti-reciprocal, a ratio of the two ordinal rates common to all arrivals from the source, which Section 8 reads as gravitational redshift. **[R]**

Picture 1 (Radar ranging)

In Bondi's radar account of relativity [13], pulses sent at a steady rate reach a receding observer at intervals stretched by Bondi's factor, the echo by the same factor, and factors of successive motions multiply. *Mapping:* Bondi's factor, a ratio of intervals $\leftrightarrow 1/\mathcal{D}$, since the Doppler factor is a ratio of frequencies; two observers exchanging pulses $\leftrightarrow$ a source and a reader exchanging counts. *Preserved relation:* the factors out and back are equal and multiply along the line of sight, and their logarithm adds as a rapidity. *Does not carry over:* a space the observers sit in before any pulse, and motion through it. *Formal statement:* the paragraph on motion above.

Readings: stretch, space and time. As candidates, the trace part of a sky's stretch, common to all directions on one reader's sky, is the cosmological redshift, a drift of the reader's tick length, and its traceless part is motion, which an isotropic drift cannot make. **[Cand]** Space as read has three dimensions, two on the sky and one along the delay; the sky is a 2-sphere because the routes reaching a reader span a lattice of rank 3 in both phases, four face-loop families before the lock and three helix families after it (Sections 2 and 3). Time as read has one, the reader's ordinal ν. **[Cand]**

Two sources, one reader. A relation between two objects is read only by a third, which knows neither source's history (Section 7): for it a coupling of two sources exists as an image $\mathcal{R} \circ \mathcal{K}$ of the sources' histories, with $\mathcal{K}$ the propagation along relay chains with their delays, by the measure chosen, and $\mathcal{R}$ the reader's demodulation, by its window, its aperture and the reader itself; with the sources fixed, the image still changes when the map does, so a distance or a motion read in the image needs none in the preimage. **[R]** It has two shapes: (I) images only, from sources that do not read; (II) a loop of images, each source reading the other and writing from a history that contains it; (I) is the limit of (II) as the histories freeze. **[R]** On the machine static seats write as in (I) (Appendix D.3). **[F+M]** (II) appears only as relay composition, witnessed by the cross term u_{12}, odd in both source signs, to which only bits that leave one seat and then the other, carrying both phases, contribute. **[F+M]** These single bits travel the shortest route between the seats, ahead of the collective mode (Appendix D.3). **[I+M]** The joint share of u_{12} grows with the reader's window against the transmission geometry (Appendix D.3). **[M]** Two scales set the image, the transmission geometry and the reader's detection window, and their ratio decides whether a joint component is read. **[I+M]** (Appendix D.3; Check D19.)

7 Readout conventions

The quaternary relation. A reading is relational in two ways. **[S]** Along one object's own ordinal it relates a present window to a past one: dynamics is this relation (the log below). **[S]** Between two objects it relates the windows of a source and of a reader, each counted in its owner's ordinal: a frame is this relation. **[S]** Together a reading relates four windows, the present and the history of the source and of the reader (Fig. 6a): the quaternary relation. **[S]** The relativity principle is relationalism (Section 1) applied to these relations: a reading uses only the causal flow passed between the four windows, never a network tick or a place on the network. **[S]** What a source emits is determined by its own history alone, and a reader compares what arrives only with its own history; neither knows the other's place or history. **[S]** Source and reader are the two ends of one causal exchange, interchangeable by the conventions below, so the principle holds alike at both ends. **[R]** The static reading is the binary limit in which the source's history freezes into structure and the reader's window grows without bound (Fig. 6b). **[I]** The CTM is no aether: a reading reads nontrivial content, what differs from the CTM, so the CTM is the datum of every reading, not a frame in one. **[R]** Reading a causal structure as physics needs conventions, since mathematics alone fixes no physical reading; here each is declared and graded, and the principles and logic bound it. **[R]** Four conventions fix what counts: a count is read at the frequency of the carrier that delivers it; a measurement compares with a recurrence; a reader is a closure with its own ruler, and readers and sources of one kind are interchangeable; and energy is the reduced Planck constant $\overline{h}$ times a count times the clock, the CTM's single swap rate. **[S]**

The transmit-receive log. A dynamical object, or any object with a period of its own, is read through a transmit-receive log: its own ordinal and its integer labels. **[S]** Motion is read against a record: a reading of motion compares what arrives now with what was written down earlier, and without the writing a reader has no history to compare with. **[R]** Writing is itself an interaction, a pen on paper, an exchange between the object and other content of the network; the machine simplifies this process and keeps only its result beside the run, as the log. **[S]** So the log is no new rule or ontology and no part of the machine's state (Appendix C): the causal order is the history, and the log implements the readout convention, as a measure does, keeping the part of the history that a reading or an emission uses, a sufficient statistic; the Kac window law below says how much history a reading needs. **[S]** It is used at both ends under the same convention: emitting, it schedules the object's own events, holds triggered by the log; reading, it supplies the reader's ordinal for the window and its references, its period for ratios of masses and its charge sign for the sign of a charge reading. **[S]** Static objects with no period of their own keep their references in frozen structure and count in network ticks. **[S]** An object's period is object data, not a tunable parameter: ratios of masses are ratios of periods, and the period is a condition of regime. **[S]**

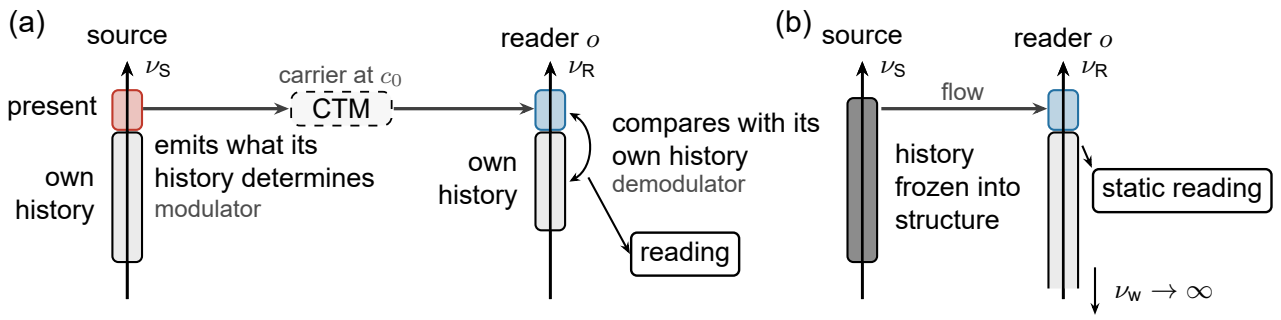

Figure 6: The quaternary relation. (a) What the source emits is determined by its own history, and the reader compares what arrives only with its own; the four windows meet only through the flow, each present a short window, not an instant; ν_S and ν_R are each owner's ordinal. (b) The static reading, the binary limit: the source's history frozen into structure, the reader's history window unbounded.

Relativity. The law layer is the relativity principle. **[S]** At the state layer, a relic bath of events, a background left from earlier eras, may rest with the overtwisted vertices, as the cosmic microwave background does, provided its drag stays below observation. **[S]** Lorentz invariance is not a property of the causal network, which has no time, length or scale of its own; it follows at readout from the relativity principle in its quaternary form, and one convention, light's speed c_0 as the conversion ratio between space and time for every reader, as the Lorentz transformation follows from Einstein's two postulates [14]. **[S+F]** Time dilation and length contraction are therefore consequences of the readout conventions, not properties of causal flow; this differs from Lorentz invariance as an infrared fixed point of dynamics [15] and from causal sets, whose order is embedded in spacetime and so must be Lorentz invariant itself [16], while here spacetime is the frame of the readings. **[R]** The criterion of relativity at the readout layer is a universal limiting speed: every reading's speed limit is the one c_0. **[R]** Given the relativity principle, the speed $\beta = |\tanh\varphi|$, in units of c_0, stays below 1. **[R]** A single bit's arrival is not a signal: only a window of the incidence transform turns arrivals into a reading, and on the network a stride is a count of cells per tick, against which "faster than light" is not defined. **[R]** The transmission-line model is the collective mode's low-k limit (Section 5), so a reader whose resolution cell is coarser than 7 cells reads an isotropic c_0. **[I+M]**

Motion: the rate law. Two models stand in for the carrier: the transmission-line measure W_{tl} carries a source's signal to a reader by the model's wave equation at stride c_0, and the identity walk measure W_{id} by Section 5's stationary walk (Appendix C).

Proposition 1 (dynamical readers and sources)**.** *Suppose that readers and sources are dynamical, as processes of content read through their transmit-receive logs, read as moving relative to the CTM, while overtwisted vertices stay seated. (i) Each counts its own ordinal ν at $1/\gamma$ times the rate of the same reader or source at rest, the rate law, with $\gamma = (1-\beta^2)^{-1/2}$.* ***[R]*** *(ii) A source whose envelope truly changes seats shows the Doppler factor $\mathcal{D} = 1/\big(\gamma(1+\beta\,\hat{n}\cdot\hat{u})\big)$, the conformal factor of the Möbius map.* ***[R+M]*** *(iii) Through W_{tl}, a source read as moving uniformly gives the Heaviside field: the transverse and axial potentials at equal distance stand in the ratio γ, there is no wake, and the reading depends only on the distance in the source's rest frame.* ***[M]***

Radar reciprocity, equal factors out and back, forces (i) (Appendix E): one tick common to all would be a clock outside the system, by which a reading would depend on who moves over the network, which the relativity principle forbids. **[R]** Proper counts, an isotropic c_0 and radar then give (ii). **[R]** For a moving reader the medium's factor times the rate law gives the relativistic Doppler factor in the relative velocity of reader and source alone, exactly in the continuum limit; lattice dispersion leaves a residual that shrinks as the reading coarsens. **[F]** The ordinal can be read at the readout layer as a two-sided Bondi count: a reader moving at β between static references fore and aft, each sending a carrier of frequency f_0 through W_{tl}, counts crests $n_\pm$ at rates $f_0(1\pm\beta)$, so $\nu = \sqrt{n_+ n_-}$ advances at $f_0\sqrt{1-\beta^2}$,

the rate law of Proposition 1(i), with no rule, the geometric mean being the reading in which the factors fore and aft are reciprocal, as the relativity principle requires; the arithmetic mean gives f_0, and one side alone $f_0(1 \pm \beta)$. **[R+F]** The run still schedules an object's own events by the rate law, through the log, as a convention; the two-sided count shows that the convention is what a reader would read anyway. **[S+M]** The Doppler factor is a frequency law: under W_{id}, a damped, partly diffusive walk, the amplitude does not carry $\mathcal{D}$, and the arrival rates compress with the right sign but not as propagation at c_0 would; under W_{tl} they follow $\mathcal{D}$ (Proposition 1). **[M]** Kinematic readings are therefore properties of the measure, built into W_{tl} and lost in W_{id}. **[R+M]** Transmission-line runs confirm (ii) and (iii) and the two-sided count within 0.5–2%; the moving reader, short of its pre-registered self-check, was not read and rests on the derivation (Appendix D.3; Checks D21–D23). **[M]**

The radar criterion. A velocity reading is the slope of a demodulated phase and must agree with the drift of the delay, and the delay drifts of one dynamical source at all seated readers must fit one timelike worldline. **[S]** In a time-invariant network, a source at a fixed place cannot produce a Doppler factor that depends on direction from frequency alone. **[F]** For dynamical sources a reading of motion needs the rate law, proper counts and an envelope that changes seats (Proposition 1). **[R]** A counterexample shows what reading the CTM would take: a reader outside the system, which the framework excludes (Section 1), timing in network ticks two references fixed on the network, one along the motion and one across, all moved over it at uc_0; both premises fail in the framework, where no reader stands outside the system and no rule moves a structure fixed on the network (Section 3), so what moves is a process of content, and readers within the system read nontrivial content, of which the CTM is the datum. **[R]** With the references d cells apart, each leg along the motion takes $d/(c_0(1 \mp u))$ ticks, and in the transmission-line model the two-way count along the motion over that across is 1.0000, 1.0197 and 1.0907 at $u = 0$, 0.2 and 0.4, within 0.09% of $1/\sqrt{1-u^2}$. **[F+M]** At the scale of a few cells the response of the CTM still runs ahead of c_0, its main front arriving early along $\langle 100 \rangle$ (D17). **[I+M]** (Checks D17, D23.)

Kac window law. A reading is a sliding-window statistic of the causal flow whose window of ν_{w} steps is counted in the reader's ordinal ν, not in network ticks, as the relativity principle forces; at the law layer the CTM could enter a reading only through a window in network ticks. **[R]** A window counted in network ticks would read ticks as time, which the network does not have, and make a reading of a dynamical source carry a factor γ. **[I]** By Kac's lemma [17], for a stationary, ergodic sequence, an event that reads j registers jointly has mean return time $\nu_{\mathsf{Kac}} = 1/\mu$ reader steps, with μ the probability per step of the required configuration. **[F+M]** For independent steps a window misses the event with probability $(1-\mu)^{\nu_{\mathsf{w}}}$, so missing it with probability at most ε needs $\nu_{\mathsf{w}} \geq \xi\, \nu_{\mathsf{Kac}} \ln(1/\varepsilon) + \nu_{\mathsf{d}}$, with ν_{d} the shortest hold and $\xi = \mu/\ln\big(1/(1-\mu)\big)$, 0.72 at $j = 1$ and 0.99 at $j = 6$ (Appendix E). **[F]** Measured windows keep this form, the Kac window law

$$\nu_{\mathsf{w}} \geq \nu_{\mathsf{w}}^{*} = \xi(j, \varepsilon)\, \nu_{\mathsf{Kac}} \ln(1/\varepsilon) + \nu_{\mathsf{d}}, \tag{5}$$

with ξ measured at $\varepsilon = 5\%$ and 1% (Table 4). Reads in sequence add their windows, joint reads multiply their return times, and the census of vertices, the count of distinguishable vertex states, does not enter. From $\varepsilon = 5\%$ to 1%, ξ rises by a common factor, so the j and ε dependences separate, but the tolerance factor is stronger than $\ln(1/\varepsilon)$: the hold-time tail is heavier than geometric (Appendix D.3). On one fixed test pattern and one torus size, the fitted $\nu_{\mathsf{w}}^{*} - \nu_{\mathsf{d}}$ grows as ν_{Kac} to the power 1.15, not 1, at both tolerances, an exponent that may carry a finite-size effect (Fig. 7); the law is this empirical bound at $\varepsilon \leq 5\%$ (Appendix D.3). **[M]** On the floor of the Kac runs, with holds off, the joint probabilities deviate seat by seat from 2^{-j} as in Section 3, a deviation fixed at each seat (Appendix D.3). **[I+M]** A reader reads non-trivial causation, content that differs from the CTM, so the deviation its own structure makes in the CTM around it is blind to it. **[R]** The runs measure a seat's holds; this paper applies the law to every window. **[S]**

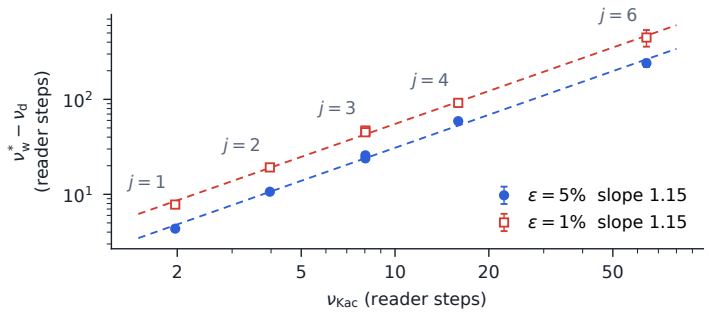

Figure 7: Coherence-window bound less the shortest hold, $\nu^*_{\mathsf{w}} - \nu_{\mathsf{d}}$, against the Kac return time ν_{Kac} of the j registers one event reads jointly ($j = 1$–4 and 6), in reader steps, for $\varepsilon = 5\%$ and 1%. Dashed lines: power-law fits.

Read-as names. In Table 1, t_{bc} is read as C and J_{state} as T. **[R]** Reading σ_d as P is a choice. **[S]** Hence CP is $t_{\mathsf{bc}} \circ \sigma_d$, on the machine $t_{\mathsf{bc}} \circ \mathrm{Rot}_2$, exact with holds. **[R+S+M]** CPT is $t_{\mathsf{bc}} \circ \sigma_d \circ J_{\mathsf{state}}$, exact on the defect-free CTM and, with holds, in distribution. **[R+S+M]** On q and h, CP and CPT act alike, T keeping both; only process order separates them (Table 1), and CPT stays in the causal order, its reversed state running forward under the same rules. **[R+S+F]** CP-odd content thus comes only from data the run places, the handedness and the defect pattern, not from the rules, as in spontaneous CP violation [18]. **[R]** The band-rotation sign h is read as helicity, the route-charge sign q as the sign of charge, and the phase weight λ as the spin weight of a readout channel: 0 for a scalar, $1/2$ for a spinor, 1 for a transverse vector, 2 for a tensor. **[R]**

Charge readings. Readings are built only from received counts, the relativity principle holds at the law layer, and all arrivals from one source worldline reach a reader with one common factor (Section 6). **[R]**

Convention 1 (ratio reading)**.** *A charge reading is a ratio of counts received from one source worldline, referred to the source's own baseline.* ***[R+S]***

As a readout convention, a charge reading does not depend on a factor common to all arrivals from one source. **[S]** A function of received counts that ignores such a factor depends only on ratios, and for a charge reading the source's own baseline supplies the reference. **[R]** For a dynamical source the common factor is $\mathcal{D}$, given the rate law of Proposition 1. **[R]**

A hold that only delays writes no static charge, since it changes a reading only at first order in the demodulation frequency ω. **[F]** This paper takes the Coulomb reading as the limit $\omega \to 0^+$, which an antenna can reach. **[S]** That limit is taken in W_{tl}, which charge readings therefore use; W_{id} serves only at $\omega = 0$, as a diagnostic. **[R]** For a source at rest both give one Poisson field up to a constant factor (Appendix E). **[F]** That fractions of a unit charge are not read is a statement of resolution, not of content. **[R]** A moving charge carries its sign in its log and stays an integer by the reader's projection onto a template of identical units. **[S]**

8 Readings

A cross reading pairs a source's perturbation of the flow, carried to the reader (Section 6), with the reader's own self-reading. **[S]** An overtwisted vertex perturbs the flow in two ways: a hold delays it, a positive count with no class sign, even under C; a turn gives it the phase $e^{i\lambda\sigma_v 2\pi/3}$, to first order imaginary and carrying the class sign σ_v, odd under C (Appendix C). **[F]** In the composed product, the reader as a scatterer, the factors multiply and their weights add; in the compared reading the reader's C-odd self-reading enters conjugated, so two $\lambda = 1/2$ responses pair into weight 0, a count (Section 7). **[S]** Conjugation keeps a real factor and reverses an imaginary one, so the compared readings

of two held sources and of two like charges have opposite signs, while the composed products share one. **[R]** Which sign attracts is a reading: by the energy convention of Section 7 the compared reading reads as an interaction energy $U(r_{12})$, with r_{12} the separation, attraction being $dU/dr_{12} > 0$: two held sources attract, like charges repel and opposite charges attract (Sections 8.1 and 8.2). **[R]** Both ride the $\lambda = 0$ kernel, which the pattern does not screen (Section 5), so both fall as $1/r$ from the source, and a closure's Gauss quantity holds, an identity of the readings, not a law of the network (Appendix E). **[R]** This fixes the signs and the shape. **[R]** How U reads for a moving reader is open (Section 9).

8.1 Mass and gravity

In the walk model the stationary weight of a held register is proportional to the inverse of one minus its hold fraction for every routing, so held content adds whatever the shape, closure length or w; by Little's law it is the Laplace slope of the $\lambda = 0$ kernel (Appendix E). **[F]** Rest mass reads as held content times the clock. **[R]** Held content is exactly additive at $\lambda = 0$ (Section 5). **[M]** Binding reads as a fixed share per adjacent A–B pair on the graph, 0.96% of one isolated overtwisted vertex (Section 5). **[M]**

A delay is a count, an always positive accumulation: the gravity cross reading is the reader's held content, a count, times the source's delay read through the reader's window as a deficit, the Laplace slope of a positive kernel. **[R+F]** The product is real, so all held content attracts. **[F]** A reading is delayed by the group delay that the static offset around held content puts on its arrivals, read as the potential. **[R]** Outside matter only one scalar remains, so the machine does not fix the light-bending parameter γ_{PPN}. **[R+M]** This paper reads the static field as the static part of a spin-2 reading, the choice that gives $\gamma_{\mathrm{PPN}} = 1$, with Fermat's principle and the Shapiro delay of a reading. **[R+S]** The anti-reciprocal ratio of ordinal rates (Section 6) reads as gravitational redshift, its logarithm a difference of potentials. **[R]** Around a held source the static offset falls as $1/r$. **[M]** The causal front and the carrier pass a held source undelayed (D4: below 4.2% of the $\gamma_{\mathrm{PPN}} = 1$ Shapiro delay). **[M]** Two held sources attract in the walk model. **[M]** (Checks D1, D2, D4.)

8.2 Charge

Read linearly in the class counts, each overtwisted vertex carries $\pm 1/3$ of a unit charge (cf. [19]), visible only to readers resolving single bands; a closed route reads its closure index w. **[R]** At $\omega = 0$ the reading is a fixed linear functional of the frozen overtwist bits, so net charge comes only from lock-written clusters unequal in A- and B-class overtwisted vertices. **[R]** Being first order in the per-vertex phase, it is not screened, as above. **[F]** No antenna reads an enclosing flux. **[R]** Seated sources and readers are placed by the run, outside the rules: their integers come only from the linear class count of unmoving overtwisted vertices. **[R+M]**

In the walk model the sign of one source's response at $\lambda = 1/2$ is a convention, since t_{bc} conjugates every reading; only products of two route-charge signs are read. **[F+M]** The compared reading has the sign $+q_{\mathrm{src}}q_{\mathrm{rdr}}$, with q_{src} and q_{rdr} the charge signs of source and reader. **[S]** The composed product is at $1/2 + 1/2$ a weight-1 frame relation, not a count, with sign $-q_{\mathrm{src}}q_{\mathrm{rdr}}$. **[F]** No C-even, rotation-invariant reading has a charge-odd part except at a charged reader. **[F]** In the walk model at $\omega \to 0^+$ the compared reading has the static Poisson shape and the sign $+q_{\mathrm{src}}q_{\mathrm{rdr}}$, so like charges repel; a charged reader reads a moving charge with the right sign, its sign carried in its log (Section 7): fed machine release events, the delay kernel gives the sign in 16 of 16 static and 8 of 8 moving cases, as W_{tl} does wherever it resolves one, though at first order that sign is nearly built in. **[M]** The walk model's shape is the reader's memory, the range of W_{id}: 2.8 cells at a memory of 50 ticks and 3.7 at 100, growing as its square root within 16%, the pattern moving it by at most 10%; the $1/r$ shape is the transmission-line reading below, where relay coupling has no scale at $p = 0$, and the pattern bounds the $\lambda = 1/2$ turning coherence (Section 5). **[M]** Under W_{tl} the structural charge reading has the Coulomb form, its exponent 1.01–1.02, and its sign agrees with the walk model in 24 of 24 cases

(D25). **[M]** Fixed test sources on the machine confirm the sign and magnitude of the composed product (D12, D13). **[M]** In the walk model a neutral reader reads only the relative sign of two sources and the dipole terms, and the lock's handedness does not enter the sign of charge. **[F+M]** (Checks D9–D13, D15, D25; Appendix E; Table 1.)

8.3 Radiation: light and gravitational waves

At $\omega \neq 0$ the channels $\lambda = \pm 1$ and ± 2, light and gravitational radiation, have degree $2\lambda\Upsilon$ and a $1/r$ radiation part (Table 2). **[R]** The network's causal flow is not light: light is the radiation part at $\lambda = \pm 1$, its two polarizations frame relations of source and reader, not CTM modes, and the carrier is the collective mode of Section 6 (cf. [3]). **[R]** Spin is the band-rotation sign h, read as helicity, with the closure sign $(-1)^w$, a sign of the image, not of particle statistics. **[R]** The CTM is not empty readout space: its cells and ticks are network units, and distances come only through the incidence transform, so the carrier's damping near overtwisted vertices (Section 5) is no dimming of light. **[R]** Overtwisted vertices on the carrier's causal paths read as a refraction mass of light, not a rest mass. **[R]** In the transmission-line model that mass vanishes where the carrier meets no overtwisted vertex; on random test patterns with lossy overtwisted vertices the quality factor is 2–7, the excitation takes from the unsigned density of overtwisted vertices a mass, the refraction mass, and its limiting stride is below c_0. **[R+M]** (Checks D3, D6, D7.)

8.4 Identical units and coherence

Species are the eigen-directions of the reader's multiplexed demodulation. **[R]** Two framed objects joined to the world by ribbons, exchanged once, are homotopic to one of them turned by 2π [20]. **[F]** A channel of weight λ gains $e^{2\pi i\lambda}$ when the frame turns by 2π, so the exchange sign is $e^{2\pi i\lambda}$, $+1$ for integer and -1 for half-integer λ: statistics belongs to the channel, not the object, an identity of the readout layer. **[R]** On the network a family 3-cycle, three turns of $2\pi/3$, carries $e^{2\pi i\lambda}$; on the CTM the $\lambda = 1/2$ sign is a gauge, -1 per bounce, a move that lands back on the vertex the bit left, with holonomy only around the fluxes. **[F+M]** The double cover is a convention of the reader's frame transport, not a measured field. **[S]** The exchange of two identical units of one class permutes the cube axes oddly and is exact only as Mir $\circ\, g$; Mir sends $e^{2\pi i\lambda}$ to $e^{-2\pi i\lambda}$, equal for half-integer λ, so the exchange sign ignores Mir, no reading is anyonic, and the chiral part $\sin 2\pi\lambda$ vanishes on every physical channel. **[F+M]** Exclusion comes from distinguishability: a minimal site carries one binary distinction, a second identical mark there makes none, so a site holds at most one elementary content (Appendix A). **[F]** The 0/1 register implements this; its variance $\rho(1-\rho)$ has the single-mode Fermi–Dirac form, read here as exclusion. **[R+F]** Identical composites of an odd or even number of $\lambda = 1/2$ constituents exchange with sign -1 or $+1$, every λ they compose having 2λ of that parity [21]. **[F]** A $\lambda = 1/2$ reading is elementary, one bit on one register, so it counts as a fermion; integer-λ readings, like the compared and composed ones, are pairs of $\lambda = 1/2$ responses and count as bosons. **[R]** Every integer-λ content may be such a pair. **[Cand]** One fact, that the elementary reading reads one bit's routing, gives both the $\mathbb{Z}_2$ sign and the hard-core count: spin–statistics is no extra postulate. **[Cand]** A composite reads as one identical unit while what a reading hands it stays below its internal gap and the reader's cell is coarser than it. **[R]** These statistics meet experiment: ^{4}He atoms bunch and ^{3}He atoms antibunch in one apparatus [22], as the parity of their $\lambda = 1/2$ constituents gives, and a neutron turned by 2π reads -1 [23, 24]; these are comparisons, not machine results. **[R]**

In causal count units the count quantum is one register mode, one bit through one register; $\overline{h}$ converts it to the reader's units. **[S]** With momentum read as $\overline{h}$ times the wave vector, the Fourier limit of the windowed transform then gives the energy–time and position–momentum uncertainty relations at $\overline{h}/2$. **[R+F]** Take a resolution cell's registers as independent and its counts as Poisson at given intensity. **[I]** Then the $\lambda = 0$ collective mode, a nearly Gaussian sum over the cell, is counted with $\mathrm{Var}\, n_c = \bar{n}_c + \bar{n}_c^2$, Einstein's fluctuation formula [25], its particle term from the count quantum,

its wave term from the Gaussian sum, and a single site with $\bar{n}_c - \bar{n}_c^2$; in second order a cell of M independent modes gives $g^{(2)}(0) = 1 + 1/M$ for the collective mode and $1 - 1/M$ for M single sites (Appendix E), seen only by a square-law or counting reader, while a linear reader of static sources reads no statistics. **[F]** On the defect-free CTM both exact limits hold, single-tick windows within 0.8 standard errors and $g^{(2)}(0) = 0$ for one register, while in longer windows the long modes' intensity moment ratio, 2 for a Gaussian, reaches up to 2.057, read as slow collective dynamics modulating their variance. **[I+M]**

In first-order interference one source reaches the reader along two relay chains, and the phase difference is the holonomy of the loop they close: ω times the delay difference at $\lambda = 0$, and at $\lambda = 1/2$ the turning holonomy, $2\pi\lambda$ per overtwisted vertex in the loop. **[R+F]** Under the identity walk measure every process that mixes a route's two directions is real and non-negative, and a hold only delays, so what makes an envelope oscillate also damps it, and at a quarter-turn phase per bounce its quality factor is at most about 1. **[F]** By Wielandt's theorem [26] a phase on a walk bounded by a stochastic one survives only if a gauge removes it. **[F]** The transmission-line measure escapes the bound: its generator is not substochastic, and at $\lambda = 0$ its lossless flux floor, the background of fluxes the pattern puts on the operator, is the identity (Section 5). **[F+M]** Interference compares two arrivals of one source's history, and its visibility asks whether the two chains' arrivals are distinguishable within the reader's resolution cell: which-path information is distinguishability. **[R]** The coherent part of the $\lambda = 1/2$ channel lives in the reader's demodulation of identical units, which it cannot tell apart: under an exact symmetry it reads them along delocalized eigen-directions, so identical seats need not be dense to be read as one. **[R+S]** Localization and coherence are complementary choices on the reader's side: the range of $\lambda = 1/2$ coherence is the screening length of Section 5, and the Kac window law bounds the resolution, the smallest readable size being about c_0 times the Kac window. **[R+M]** In the walk model a sign per bounce is a gauge that removes the phase, while a quarter-turn phase per bounce dephases at the bounce rate (D28). **[M]** A pilot with three identical seats reads them as a symmetric mode and a doublet at $\lambda = 1/2$ and as separate seats at $\lambda = 0$, the coupling not resolved from zero (Appendix D.3). **[M]** A velocity reading arises when readings change seats: in the line model (Appendix C), a coherent, densely packed boundary of identical units, read as moving below c_0, passes the radar criterion and a non-identical one fails, the precursor of the processes of content of Sections 6 and 7. **[M]**

The compared cross reading has a C-even part E_+, the C-even component of phase coherence in the turning channel, second order in Φ through $\cos\Phi - 1$; it factorizes as the source's even field times the reader's real self-reading, has one sign for every pair of charges and takes its sign from the reader. **[R+M]** It carries the same $1 - \cos\Phi$ as the screening of coherence. **[I]** (Checks D8, D15, D16, D18, D24, D25–D28.)

8.5 Cosmology

The network tick n reads as conformal time η; the only conversion that drifts is the reader tick length b, in network ticks. **[R]** A reader cell, the cell a reader resolves, holds b^3 network cells, so its held content dilutes as b^3. **[R]** Read through the Friedmann equation of general relativity, in the continuum limit b obeys $(db/d\eta)^2 = \mathcal{C}_\Lambda + \mathcal{C}_m b^3$, with $H = -db/d\eta$, in which Λ is only a first integral (cf. unimodular gravity [27, 28, 29]). **[R]** The vacuum, the CTM's readout name, has a held level, its held content per reader cell, which enters $\mathcal{C}_\Lambda$ as a share in reader units; per network cell it would dilute as b^3 and be matter. **[R]** If a dimensionless mass ratio depends on the CTM's noise amplitude, mixing must end early, or a fine-grained transition density still changing late would break the bounds on a drift of the proton-to-electron mass ratio. **[Cond]** The scale factor $1/b$ increases and is convex in conformal time in every era (Appendix E), so it never saturates, and the bounded, saturating mixed fraction cannot be it. **[R]**

In the continuum limit the Λ era ends with b falling linearly to zero at a finite η_∞, and deep in that era $H_\Lambda^{-1} = (\eta_\infty - \eta)/b$, the future still resolvable in reader ticks, stays constant. **[R]** In reader time t

the approach $H^2 - H_\Lambda^2 \propto \exp(-3H_\Lambda t)$, to leading order, is a tail whose fixed point in the continuum limit is de Sitter. **[R]** The knee $H^2 = 2H_\Lambda^2$, where the tail begins and the held content of a reader cell falls to the held level, is by definition the matter–Λ equality. **[R]** If a reader tick is at least one machine step, a finite machine saturates: H falls to zero, and the event horizon disappears. **[R]** Taking this as the end state, beside the eternal H_Λ of the continuum limit, is a choice. **[S]** If Newton's constant is a number times a cell area, that cell is a reader-side screen cell of fixed area in reader units, since a network cell would drift at twice the Hubble rate, beyond observed bounds. **[Cond]** (Appendix E.)

9 Open problems and future work

Open: the content dynamics, under the rules as given, that carries a moving reader or source across the fixed pattern, with an explicit tick-to-tick transfer of the transmit-receive log that Section 7 keeps by convention; the consistency of U as read by a radially moving reader; and the integral of its frequency shift against the change of U (Section 8).

A reader whose window nears the coarse-graining scale of about seven cells, some 50 ticks at c_0 or 100 for a two-sided window, resolves causal bits at about $10^2\overline{h}$ in count units and could read the network before coarse-graining: the collective mode's dispersion, its anisotropy and the early $\langle 100 \rangle$ front (Sections 5 and 7). Under which experimental conditions a reading reaches this scale is open; it would read the structure beneath the readout conventions, not a failure of them.

The pattern is primordial data (Section 3): where integer charges sit, how thirds are confined, the structures that fill the vacuum and the statistics behind the microwave background go to the sequel.

The law-level zero $\langle q \cdot h \rangle = 0$ belongs to the routing layer, its structure and rules (Section 4). The weak and strong readings belong to the readout layer and lie outside this paper's scope, and with them stay open the weak interaction's chirality; observed CP violation, in kaon and B-meson systems, and the baryon asymmetry, both resting also on the pattern; particle scales; generations; and the held level. Holding delays the causal flow for every reader, up to the conversion of scale: this is the network form of the equivalence principle, which the Eötvös experiments check at the readout layer; how to measure it on the machine for readers of every kind is open.

10 Conclusion

This paper builds one causal network on a fixed graph, a purely mathematical structure, and studies it through the routing machine that implements it. The epistemic principles give the network its form, criteria read from them select its graph, the Laves graph on a three-torus, and its rules have no tunable parameter: their constants are structural or declared, none continuous. Appendices A and B record how the principles lead to this graph and how the lock writes its bands; they supplement the construction rather than carry the paper's central claim, for every reading is taken from, and checked on, the machine as given or its linear models (Appendix C). What the network is read as comes from declared conventions; the code, its tests and the hashed run records are released, and each reading of Section 8 has its check (Table 3).

Pieces known from separate fields reappear here as rules or readings of this one machine. Its principles take distinction as the primitive act, as in Spencer-Brown's calculus of indications [30]; before the lock its rules are deterministic and reversible, as in the automata proposed beneath physics [31, 32]; a release forgets its entry band, the erasure at the root of irreversibility [33], and so writes the arrow. Coarse-grained, as in hydrodynamic limits [34], the flow carries the sound mode of lattice gases [8, 9], measured at c_0, and the CTM among unmoving overtwisted vertices is a gas among fixed scatterers [35, 36]. On the reader's side, Bondi's radar account [13] returns in the Doppler factor of dynamical readers and sources; the measured window law rests on Kac's recurrence [17]; CP-odd content is read from data, not rules, as in spontaneous CP violation [18]; charge thirds are read at overtwisted vertices, as twists on ribbons carry them [19]; Λ is read as an integration constant through

the Friedmann equation of general relativity [27, 28, 29]; the belt trick gives the exchange sign [20]; Einstein's fluctuation formula returns for the collective mode [25]; composites follow the parity rule of their constituents [21]; and, as candidates, motion is the traceless stretch of the reader's sky and the arrival frames form the Hopf fibration over it. Because all of these are rules or readings of one machine, they hold together in one self-consistent mathematical frame whose consistency can be run on it, each claim graded and each measurement checkable: this integration is the paper's significance.

The construction joins the programs that look beneath spacetime geometry: pregeometry [37, 38], spin networks [39], causal sets [40], digital physics [1, 2], hypergraph rewriting [41] and quantum graphity [42]. What it adds is a fixed graph, on which no rule adds or removes a vertex or an edge; one machine whose readings can be run; and relativity entering once, at readout, as relationalism taken apart into a quaternary relation of dynamics and frame, from which, with c_0 as the conversion ratio between space and time, the Lorentz transformation follows, checked in part: a moving source shows $\mathcal{D}$ in the transmission-line model, one-way Doppler readings depend on the relative velocity alone by derivation in the continuum limit, and a two-way radar counterexample shows that only a reader outside the system could read the CTM. Section 9 names what stays open, above all how to measure on the machine that holding delays the causal flow for every reader.

A Principles and the construction of T^3

A.1 Principles

This subsection fixes the principles' working form, to which **[F]** and **[R]** refer. Finiteness refuses infinity, so compactness is forced and the information budget sealed. Distinguishability admits only what can be distinguished. Minimal sufficiency adds only rules that unlock new readable content, a distinction no local rule could read before. These premises carry no grade: they are epistemic, taken rather than provable inside the theory.

Finiteness seals inflow only: nothing enters from outside, erasure is allowed, and compactness orders no events. Distinguishability takes two steps, a mark against no mark, then the mark's two sides defining each other, so which value is called 1 is a gauge; before the lock no rule tells the values apart, so rules commute with X (Section 4), and the occupancy $1/2$, this symmetry read, persists, as a later stage does not dismantle an earlier category. The lock names the values by the handedness of its half twists, one undetermined bit chosen before the lock. Distinguishability also drives the construction (the drive) while a local rule can still unlock a readable distinction; Minimal sufficiency drives nothing and cuts rules, not implementations. **[R]** The lock unlocks a contrast between vertices, so the irreversible cut runs between vertices and events live on venues. **[R]** On a band this is forced: crossing an untwisted band as if untwisted is the identity. **[F]** At a vertex it is a reading: a vertex not overtwisted hosts no event. **[R]**

The network stores no coordinate, since a position label would enter from outside and no rule reads an ambient manifold; no shared clock, since a free choice would enter from outside and a second writer would make outcomes depend on update order, hence one writer per register and confluent rules; and no field, since a register holds one unnamed binary distinction, so before the lock the state is occupancy alone. **[F]**

A.2 Lemmas on local maps

Four lemmas bound the local maps; the first three rest on exhaustive enumerations of the maps (Data and code availability). Distinguishability restricts a local rule twice: before the lock it commutes with X, and it reads every input, an unread input being gauge. **[R]** *Two-input lemma*: a map from two input to two output registers is a bijection, one of eight that pass or cross the bits, each with one of four bitwise complements. **[F]** *No-merge lemma*: none of the eight reads its inputs jointly, merges two inputs or writes an output from none. **[F]** *Three-input lemma*: of the eight maps on three registers that

also commute with every permutation of the bands, four are not injective: majority or parity on every output, and their complements. **[F]** *Routing lemma*: routing read from the bands moves each bit along a curve with one successor at each point, so it permutes the registers for any twists and overtwisted vertices. **[F]** The open premises are one register per input, where the machine has six entry registers per vertex (Appendix C), and one reader per register.

A.3 Construction of the three-torus

The principles build a zipper of degree three on a circle, and criteria read from them select the Laves graph on T^3. A distinction has one successor and one predecessor, a bijection on a finite set and a single cycle if connected; a segment's ends would have degree one, against one rule everywhere, so the first object is a circle. **[F]** Its second side, fixed by the first since inflow is sealed and differing from it for both values, is its complement, so every mirror pair holds one 1 and no information is added. **[F]** By the no-merge lemma this two-way circle unlocks nothing, so the drive adds the least structure giving every vertex three inputs, one chord per mark, an edge joining two marks that closes the circle like a zipper, and degree three is the first at which a rule can read content (three-input lemma). **[F]** A cyclic order chosen vertex by vertex would let one bit per vertex in, so one rotation system holds everywhere. **[I]** The three band families give at most three independent directions; isotropy and the families' independence are the criteria. **[R]** Under each of the eight rotation systems the zipper's labels fix, a direction-keeping walk finds the two-pitch net (a pitch is a chord's offset along the circle) anisotropic by about a factor three, while the Laves graph is isotropic under the rotation system uniform in the band families, so the criteria select it. **[R+M]** The Laves graph is such a zipper, of period eight with four pitches, two sizes each used once in each direction. **[M]** The number of marks and the zipper parameter, the first chord's offset, set its chord sizes and so the size of T^3. **[R]** The three-torus is the flat, finite, unbounded and minimal compactification: other orientable flat ones glue with a rotation, one more rule that would permute the route families around a cycle, which Minimal sufficiency cuts. **[I]** Why the period is eight is open.

A.4 Where irreversibility sits

Five steps, using no machine rule, put every irreversible event at an overtwisted vertex. Irreversible events exist: halting while a local rule can still unlock an arrow violates the drive. **[R]** The lock leaves overtwisted vertices: writing only a uniform twist is injective, and a distinction between dwelling and passing needs both sides non-empty. **[F]** No renaming of sides removes the lock's half twist on every band, so every band is a venue for the swap, its own inverse, and holds on bands are excluded, since the irreversible cut runs between vertices. **[F]** Plain vertices host no event and only route, which permutes the registers. **[F]** Every update off overtwisted vertices is thus a bijection, and irreversible events and held states sit only at overtwisted vertices. **[F]** Whether that event is a hold is the machine's choice (Appendix C). **[S]** The open premises are the lemmas' (Appendix A.2).

B Band topology and the lock

None of this appendix's results assumes a particular pattern of overtwisted vertices.

B.1 Bands, sides and framing

Before the lock a band's two strands must be its sides: an untwisted band keeps each bit's side, so a strand that changed sides would be no flow line, and a full strand beside an empty one could not mix under rules conserving both strand counts. **[F]** Counts are conserved side by side before the lock and strand by strand after it; only the occupancy $1/2$ carries across to χ. **[F]** A half twist crosses a band's sides once and so reconnects the routes: untwisted, routes circle faces; twisted on every band, the

turns alternate and routes run straight as Petrie walks, so the uniform twist is Petrie duality [43], whose walks are exactly the routes of untwisted bands with every B vertex, or every A vertex, overtwisted, related cycle by cycle by $s \oplus [u \in \mathrm{B}]$. **[F+M]** Writing on the bands is thus the only writing that picks no class, and a vertex carries no invariant beyond its bands' twists. **[F+M]**

At the isotopy layer, with straight bands and flat vertex discs, a contractible cycle's framing is its base value plus half the sum of τ_e over its bands; all 324 ten-rings of the three-cell torus have full rank, so no gauge remains, and on a theta graph, two ten-rings sharing one band closed by a contractible eighteen-ring (Fig. 4c), framings counted from base values give $\mathrm{Fr}_1 + \mathrm{Fr}_2 - \mathrm{Fr}_3 = \tau_e$. **[F+M]** At the homotopy layer only the framing mod 2 survives, one $\mathbb{Z}_2$ flux per ten-ring. **[F+M]** A pinch (Section 4) takes τ_e from 1 to -1 and conserves no framing, so conservation could only be declared by a rule. **[F+M]**

B.2 The routes of the two phases

These counts back the route claims of Sections 2 and 3 and Fig. 2. A face loop uses each band family once per period, and three of the four face-loop families meet at each vertex; after the lock each vertex lies on one helix of each axis family; on the machine's realisation the face loops are right-handed and the axis helices left-handed. **[M]** No route of either kind is contractible on the torus, and both phases span a lattice of rank 3: the twist changes the families, not the dimension. **[M]**

B.3 The band embedding of a defect

On the band of an adjacent overtwisted A–B pair the three half twists of Section 3 are invariant for the fixed embedding: they and the alternative single one differ by a full turn, which flips the sign of a route crossing once; the band's ends join other bands, so no belt trick removes the turn, and by the Călugăreanu–White–Fuller theorem each cycle through the band keeps $\mathrm{Lk} = \mathrm{Tw} + \mathrm{Wr}$. **[F+M]** The embedding does not fix the content the lock leaves; where the reconnection sits relative to content in transit does. **[F+M]**

B.4 The lock process

Twists written between ticks never mix: an untwisted band keeps the sides, and a twisted one then holds a side of 1s against a side of 0s, so its swap changes nothing and no hold can capture; the side-ordered start, one side of every band all 1s and the other all 0s, is a fixed point under any history of twists, defects included, and either labelling of content. **[F+M]** With the venue of Section 3, the twist must therefore be written while content crosses the band. **[F]** Routing sees a new twist in the tick it is written, swap detection, which runs first, a tick later, so each band's first twisted crossing is unprotected. **[F]** Routing reads $g_e = \tau_e + \mathrm{rot}_u + \mathrm{rot}_{u'} \bmod 2$ for band e with ends u, u', so one more half twist on a vertex's bands reverses its turning and leaves routing unchanged, and turning left or right and being plain or overtwisted are one bit; holds read f_u (Appendix C). **[F]** Of the sixteen occupancies of a band's four entry registers, exactly two give different outcomes with and without the twist while changing no strand count; there the swap fires, crossing as if untwisted wherever that is safe for χ. **[F]**

B.5 How the mixing opens

The mixing opens at the twist front, at each band's unprotected first crossing. With no overtwisted vertex, a twist written everywhere at once complements every register's side order, and nothing mixes. **[F+M]** With overtwisted vertices written on their bands, it mixes, starting from them. **[M]** One freshly twisted band on the side-ordered start is, register by register, a single content seed. **[F]** Behind a front from nucleation points, content at a band mixes within a few ticks of the twist's arrival, the composition follows the part of the network the front has not reached, with no dynamical long tail,

and the density of transitions holds at $1/2$ (Appendix D, D5). **[M]** How long the mixing lasts, and the shape of its tail, depend on the pattern and are left to the sequel. **[F+M]**

B.6 A seat's several pasts

A seat's update merges states, so a held state has several pasts: at an isolated overtwisted A or B vertex with the rest of the flow empty, the 256 states of its six entry registers and its buffer have 211 successors. **[F+M]**

C Machine specification

This appendix specifies the routing machine of Section 3 as its code release runs it. The code calls a band an arm and its number $m \in \mathbb{Z}_3$ (Section 2) its arm index.

C.1 The routing machine

State and tick. Each vertex carries its class (Section 2) and its overtwist bit f_u, which the lock writes. By design f_u stays fixed after the lock, and content is six entry registers per vertex, one on each side of each band, holding 0 or 1 with no label; the two sides per band are not derived. **[S]** Readers, their windows and their transmit-receive logs are readout conventions implemented on the machine's state, not part of it (Section 7). **[S]** Each overtwisted vertex has one routing buffer, empty or holding one pair, one χ_1 and one χ_0. **[S]** A tick runs, in order, the buffer step, swap detection, the swaps and the routing. **[S]**

Venue and routing. A swap fires only on a venue, a band with $\tau_e \geq 1$, the bands of an overtwisted vertex included. **[S]** Admitting only odd τ_e would bar swaps on the bands with one overtwisted end and on no others. **[F]** The code routes in the gauge $\mathrm{rot}_u = f_u$, every written band read as one half twist: a bit entering on slot m at side s leaves on slot $m + (2s-1)(1-2f_u)$ mod 3, and g_e equals its value in the gauge $\mathrm{rot}_u = 0$, $\tau_e = 1 + f_u + f_{u'}$. **[F+M]** On a band the lock has not yet written, a bit keeps its side.

Swap. On a venue the swap fires when both registers on one side of the band hold 1 and both on the other hold 0, or all four hold 1 (occupancy unchanged), and the bits then cross as if untwisted (Appendix B.4). **[F]** Bits released in a tick take no part in that tick's swaps. **[S]**

Hold and release. An empty buffer captures a pair when an entry register on one band of the seat and its mirror partner are both occupied, not counting registers just filled by a release. If two bands qualify, it captures on the one after the other band in the seat's turning sense, that of χ_1 at a plain vertex of its class; if three, none. At each tick the held pair is offered to its exit band, at first the band of capture: if both entry registers of that band are empty, the pair is released into them and routed, and otherwise the exit band moves one slot on in the turning sense. **[S]** Failed offers set where the bits leave (table below). A routed exit is the one a bit would take unheld.

Failed offers, mod 3	χ_1 leaves by	χ_0 leaves by
0	routed exit	routed exit
1	entry band	χ_1's routed exit
2	χ_0's routed exit	entry band

The entry band need not be stored: it is the exit band moved back by the failed offers, so the engines store only the exit band. **[F]**

No rule has a tunable parameter: the constants of a tick (three bands, two sides, one pair per seat, the turning sense) are structural, some declared choices, none continuous; the pattern, the initial content and the front's schedule are inputs of a run. **[F]**

C.2 Engines and tests

The reference engine steps on the Laves graph with these constructor and buffer tables and a capture tie rule. **[M]** A vectorised fast engine agrees with it bit for bit, content, held exit band and tags at every tick, in 90 runs (2- to 4-cell tori; no overtwisted vertices, shares 0.05 and 0.3, adjacent A–B pairs, a fixed test pattern; $\rho = 0.3$ and 0.5; three lock masks: none written, all written, random). **[M]** Each tick the reference engine asserts the bit count, single occupancy and, once every band is written, both strand counts. **[M]** Both classes agree with the failed-offers table at 32 A and 32 B seats on a 3-cell torus, 1152 cases. **[M]** On 3- and 4-cell tori with overtwisted share 0.3 and random content at $\rho = 0.3$ and 0.5, 48 asynchronous schedules with holds and swaps on agree with the synchronous run bit for bit, and a band update that does not wait for both its ends fails in 24 of 24. **[M]** The code release holds 5 test files with 136 checks, all passing. **[M]**

C.3 Linear models

Three linear models stand beside the machine; each is specified here as its code runs it, and these descriptions carry no grade.

Walk model. The walk model, measure W_{id}, lives on the machine's registers, six per vertex, on the Laves graph, built as the cubic srs net. In one tick a walker follows its route with probability $7/8$, changing side across the half-twisted band, and takes a swap with probability $1/8$, the single-swap rate per bit per tick at $\rho = 1/2$, its identity following either swapped bit with equal weight; the routing-and-swap matrix is doubly stochastic. Each step survives with probability e^{-m}, $1/m$ ticks being the reader's memory: $m = 0.01$ in most readings, 0.003 and 0.0025 in two far-field and charge runs, and 0.02 for D15 and D25. A move out of a register at an overtwisted vertex carries the class-signed phase factor $e^{i\lambda\sigma_v 2\pi/3}$, with $\sigma_v = +1$ at A and -1 at B, $\lambda = 1/2$ for charge and $\lambda \to 0$ for linear response. Holds are delays: at each register of an overtwisted vertex the walker stays with probability κ_u per tick and otherwise moves by the routing-and-swap matrix; the paper's runs set $\kappa_u = 1/2$ at every overtwisted vertex, $1/4$ to $3/4$ in two checks, and read the hold channel at $\lambda = 0$. Three evaluation forms are used: the exact sum over all walks, by an iterative linear solve; a power series truncated at 300 ticks, with survival $e^{-m+i\omega}$ at demodulation frequency ω and truncation error e^{-300m}; and a retarded, time-resolved sum, each event entering at its tick. A reader at a vertex reads the mean over its six registers, a reader of several vertices the mean of these means, on a periodic torus with minimum-image distances and no image correction.

Transmission-line model. The transmission-line model, measure W_{tl}, has no registers, sides or routing: its field ψ lives on the edges of the net, twelve per cubic cell, and at each vertex three hops couple its edges in pairs, every edge meeting four hops. With $\mathcal{L}$ the sum of squared differences across hops, $\ddot{\psi} = -c^2\mathcal{L}\psi$ plus a source term is integrated by leapfrog with a step of half a tick, $c = 4c_0$ giving the small-k dispersion $\omega = c_0 k$; the static limit, $c^2\mathcal{L}\psi$ equal to the source, is a Poisson problem solved by conjugate gradients. At an overtwisted vertex the hops carry the turn-signed connection $e^{-2\pi i\lambda/3}$, with no class sign, so each such vertex holds a flux -1 at $\lambda = 1/2$, a π flux; $\mathcal{L}$ with these fluxes is the flux floor, whose lowest eigenvalue is the gap Δ of Section 5. The class sign enters through the source: a static unit source is split over a vertex's three edges and neutralised, its mean removed, a structural charge source weights its vertices by $\sigma_v/3$, and a static reader reads the mean of the field over its edges. Time-domain runs use Gaussian source and reader kernels on edge midpoints, 0.5 to 1 cell wide, a source switched on over 128 ticks, a weak uniform damping $\gamma_0 = 0.08\, c_0$ per cell and absorbing sponges beyond 16 to 19 cells; windows are applied in the analysis, not in the model. The lossy variant behind D3 is a separate first-order code, with loss on the three hops of each overtwisted vertex and its stride and loss taken from the machine's coarse-grained table.

Line model. The line model, a mechanism diagnostic with an imposed front, not machine dynamics and not on the net, is a one-dimensional telegraph line in units of c_0, a density on 3800 sites and a current between them, advanced by a staggered leapfrog with sponge ends. Its units are loss pixels from site 600 on, identical shunt losses every second site or sparse, random or jittered ones; the imposed front lights the pixel at x at the time $(x - 600)/u$ after the start, its response rising and falling over 4 ticks, and a frozen reader at site 300 sends a probe and reads the echo as the record with pixels minus the record without.

Relation to the machine. The transmission-line operator is the lossless low-k limit of the machine's collective mode at $p = 0$: both run at $c_0 = v_{\text{bit}}/\sqrt{3}$, and the mode's stride comes within 0.24% of it as $k \to 0$ (D7, D17). **[I+M]** At $p > 0$ the mode is lossy: with lossy overtwisted vertices the quality factor is 2–7 (D3). **[M]** The r^2 image term in static fits on the torus is an analysis-side correction, not part of the model, and the fitted Coulomb exponent depends on the fit's weighting (D25). **[M]**

D Methods and machine check table

D.1 Check table

Table 3 gives, by the section whose claims it checks, each check behind a measured claim, with its number, measured in the model the row names; the deposit README maps each key to its check module, its producers and its records; a pilot rests on fewer than six seeds, and a failed pre-registered rule is stated in its row; what failed is not a claim of this paper. **[M]** On one laptop CPU core the reference engine advances 4.1–4.7×10^6 vertex-ticks per second and the vectorised engine 1.5–1.6×10^7 on 8- and 16-cell tori, eight vertices per cell; the check stages run in seconds to minutes, the largest in about half an hour, and the longest producer in about two hours. **[M]**

Key	Model	Check	Number
Section 4			
D16	M	parity law, every proper isometry	23/23 classes, 48/48 cosets; both forms exact with no overtwisted vertex
Section 5			
D7	M	collective-mode stride, one mode driven	0.1444–0.1445 cells per tick along $\langle 100 \rangle$ at $k = 0.262$, 24- and 48-cell tori (predicted $c_0 = 0.1443$)
D17	M	dispersion and damping, $p = 0$	$c(k \to 0)$ within 0.24% of c_0; z = 1.87–2.15; set after w155, w155b failed their rules (single-cell response 4–13% ahead of c_0 at 4–22 cells)
D18	TL, W	flux-floor screening; $\lambda = 0$; walk-measure range	$\ell \propto p^{-0.54}$; $\lambda = 0$ to 2×10^{-11}; pre-registered "extinction" rests on a window-limited point; walk range 3.7 cells at 100 ticks, square root of memory within 16%
Section 6			
D14	W	fibre angle at a reader; $\lambda = 2$ against $\lambda = -1$	four fibre values, only 0 on the lattice; magnitudes differ by 16–30% rms over sky bins, equal for the lattice angle
D19	M	two sources: captures, relay, image	< 0.04 captures per release, relay excess ≤ 2.65 (pilots, two seeds); reader factor 1; joint share rising with the window (Appendix D.3); switching rule 2/4 in the pilot, 4/4 at six seeds; switch-on 8–13.5 ticks after switch-off (1.7–5 s.e.)
D20	TL	beamforming, pilot	bias $\leq 2.4°$ in 18/18; width 6/6, proportionality missed by 0.03; one-vertex flatness failed 3/14
Section 7			
D21	W, TL	moving charge sign; Doppler	sign 16/16 static, 8/8 moving; $\mathcal{D}$ within 2% at β = 0.3, 0.5 (w156 v2); failed: w140's estimator, w156 v1's static reference, w156 v2 static reference 0.25% against a 0.2% rule
D22	TL	two-sided count	within 0.8% at $\beta = 0.6$; axes agree within 0.19% at $\beta = 0.3$ and 1.09% at $\beta = 0.6$, against a 1% rule; 0.06–0.32% with references at 3 cells

Table 3, continued

Key	Model	Check	Number
D23	TL	two-way radar (counterexample); co-moving Doppler	radar within 0.09%; co-moving self-check within 0.15%, failed 3/12 at the 0.1% gate, stop rule fired
Section 8.1			
D1	W	$\lambda = 0$ reading of held sources	-0.057 to -0.059 per overtwisted vertex, any w or shape
D2	M	held content, 36 constructed sets	$-0.96\% \pm 0.06\%$ of an isolated overtwisted vertex per adjacent A–B pair
D4	M	offset, front and carrier delay, held test source	offset $\propto 1/r$ to 2%, r = 3.5–44 cells; front shift 0 ± 0.26 ticks; carrier delay $\leq 4.2\%$ of the $\gamma_{\text{PPN}} = 1$ Shapiro delay, every bin within 1.5 s.e. of zero, impact parameter ≥ 1.5 cells
Section 8.2			
D9	W	linear charge response	14-vertex closure : A vertex : A–B pair $= 1 : 0.337 : 0$; first order to 1.5%
D10	W, TL	Gauss quantity; outward flux	equal on three balls and a box; flux 0.9999–1.0000 at radii 5–7 cells (TL)
D11	M	held signs imposed, fixed test unit	$1/e$ decay in 0.75 ticks; no hysteresis
D12	W	t_{bc} against conjugation; composed reader sign	equal to 3×10^{-16} at $\lambda = 1/2$; $-q_{\text{src}} q_{\text{rdr}}$ at 48/48 shell points
D13	W, M	composed Poisson sign; neutral reader; machine, fixed test sources	42 560/42 560 placements; 5517/5517 per setting; 24/24, at 9–24 s.e.
D15	W	compared cross reading	sign $+q_{\text{src}} q_{\text{rdr}}$ for the source-odd reading (24/24 A, 24/24 B); held sources negative, 48/48; at $\omega = 0$, 0.94 and 0.99 of the composed value, and the source-even part E_+ about 0.9 of the odd part, positive for both readers, removed by the odd projection
D25	W, TL	attraction signs; Coulomb form; E_+	signs of Section 8, range 2.8 cells (walk); exponent 1.01–1.02, up to 1.10 weighted to the far shells; signs 24/24; E_+ rank one to 2%
Section 8.3			
D3	TL	lowest mode, random test patterns, $p = 0.0025$–0.08	mass $\to 0$ as $p \to 0$; lossy: quality factor 2–7
D6	M, W	frame-loop sign; $\lambda = 1$ frames	$(-1)^w$ on all 3054 closed routes to length 20; $\lambda = 1$ blind to routing
Section 8.4			
D24	M	identical seats, pilot	doublet, reader weight 0 at $\lambda = 1/2$; separate seats at $\lambda = 0$; w142 (eight seeds): $\lambda = 1/2$ coupling not established, its rules failed
D26	M	bunching limits on the CTM, cells of 48–3072 registers	within 0.8 s.e.; one register 0; windowed ≤ 2.057
D27	TL, M	holonomy of the λ medium, pilot; family 3-cycle	$2\pi\lambda$ per overtwisted vertex; windings 0; 3-cycle collects $e^{\pm 2\pi i \lambda}$, $J = 0$ on the bare net at $\lambda = 1/2$ and 1
D28	W, M	envelope under the walk measure; flat lifts	bounce sign a gauge; quarter turn dephases, quality factor 1.07; all 8 flat lifts put -1 on every bounce
D8	L	dense identical boundary lit in sequence	Doppler equals delay drift to 0.002, β = 0.3–0.98; sparse, mixed or superluminal fail
Appendix B.5			
D5	M	fronts from fixed test seed sets	99.5% mixed 8 ticks after the twist; late composition $1/2$ to 10^{-3}

Table 3: Checks by the section whose claims they check. Model (Appendix C): M machine, W walk, TL transmission line, L line. wNNN: a research run that a key's check module was ported from; the deposit README names the module.

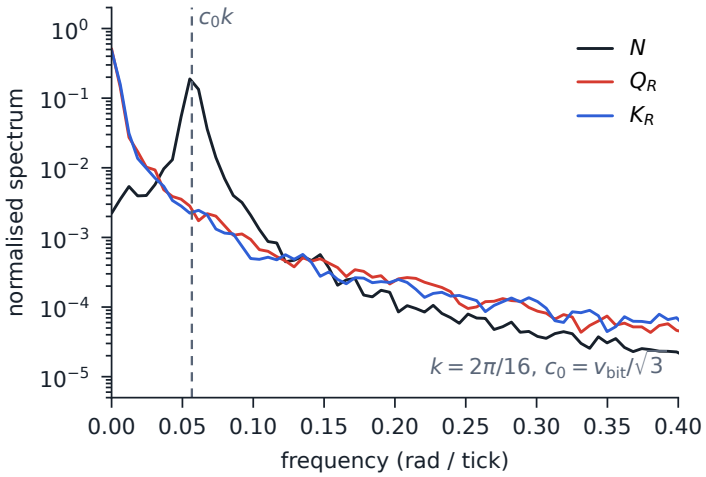

Figure 8: Spectra of the densities N, Q_R and K_R on the CTM at wavenumber $k = 2\pi/16$ along a cube axis (16-cell torus, 1024 ticks, four seeds), each normalised to its sum. Only N has a peak, at frequency $c_0 k$ (dashed), with $c_0 = v_{\text{bit}}/\sqrt{3}$, while Q_R and K_R carry their weight at zero frequency.

D.2 Coarse-graining on the machine

Route charges and the collective mode. On an 8-cell torus the 384 routes keep their Q_R through 200 ticks and 153,020 swaps, and at $p = 0.01$ with holds on, the 40 overtwisted vertices each merge three routes into one, and the 304 routes keep theirs through 1521 captures. **[F+M]** On the same torus none of the K_R changes in 300 ticks. **[M]** Driven one mode at a time, the machine gives 0.1444–0.1445 cell per tick along $\langle 100 \rangle$ at $k = 0.262$ on 24- and 48-cell tori, against $c_0 = 0.1443$. **[M]** Driving four modes at once slows it by up to 1.1%, read as the second-order drift effect (Section 5). **[I+M]** For a lattice wavevector along a cube axis, both transverse components of $\mathcal{P}$ stay frozen, with correlation 0.99 after 512 ticks on a 16-cell torus. **[M]** At drift $0.27\,c_0$ the machine splits the strides along and against the drift by $-0.003\,c_0$. **[M]** The machine matches the linear prediction of Eq. (4) for the second-order anisotropy to three digits at the smaller drift and to about two at the larger (Appendix E). **[M]**

Spectra. In the spectra of Fig. 8, N peaks within one frequency bin of $c_0 k$ at 85 times its zero-frequency value, while Q_R and K_R keep 85% and 86% of their weight near zero frequency and have no peak. **[M]**

Sinks. A causal flow drifting over the overtwisted vertices loses lattice momentum at 0.13–$0.14\,p$ per tick with holds off and 0.19–$0.20\,p$ with holds on, as a fraction of the initial momentum over ticks 2–40 (16-cell torus, two seeds, $p = 0.0025$–0.04; $0.129\,p$ on a 24-cell torus). The measured decay is not exponential: with holds off the loss collapses onto one curve in $p\sqrt{n}$ over the network tick n, with a power-law tail $\approx 0.5/(p\sqrt{n})$, and three arrangements of the overtwisted vertices change it by at most 5%, on tori up to 24 cells. **[M]** A fractal arrangement is untested.

Drag and modulation. A closure of 14 vertices with seven overtwisted vertices, moved through tori of 24 and 32 cells at 0.25 to $1.5\,c_0$, drags at most 7×10^{-4} of its gross exchange, the bits it trades with the CTM per tick, each value within about one standard error of zero (4–8 seeds, 160–240 ticks). Holds that only delay also give zero drag. **[M]** Irreversibility is necessary but not sufficient: on a clean 16-cell torus (four seeds, 160 ticks), labels, markers advanced along a lane, trigger holds at the nearest seats, and holds that only delay drag by at most 0.0017 ± 0.0013 bit momenta per label per tick, 1.0% of the gross exchange, against 0.032 to 0.048, 16–21% of it, for an irreversible release that changes band with the direction of motion. In a drifting causal flow a reversible object is itself a sink of lattice momentum. **[M]** On a fixed test unit, one chosen cluster of overtwisted vertices, the machine confirms Theorem 2: each class run alone under period-2 routing equals the static pattern

with that class overtwisted and holds gated, bit for bit over 400 ticks in six trials; under period-3 routing no line exceeds 1.3 standard errors at $2\pi/3$ without holds, while holds write a phase-locked line of 27 standard errors in the capture rate, 4% of its mean (8-cell torus, 24 seeds of 8000 ticks). **[M]**

Static readings. In the walk model on a 12-cell torus the reading is 0.985 to 0.989 of the additive value, the deficit scaling with the killing rate. **[M]** In the walk model the three-dimensional winding number falls from 8×10^{-4} to 2×10^{-5} as the grid is refined. **[M]** On a fixed test pattern, trails of three and seven vertices read 1.503 and 1.545 in magnitude, a finite-length correction of 2.8%. **[M]**

Dispersion and damping. At $p = 0$ the dispersion $\omega(k)$ and decay rate $\Gamma(k)$ of the collective mode are fitted to the equilibrium time correlation of N at each wavenumber k (48-cell torus, six seeds). As $k \to 0$ the stride ω/k is 0.1443, 0.1447 and 0.1442 cell per tick along $\langle 100 \rangle$, $\langle 110 \rangle$ and $\langle 111 \rangle$, against $c_0 = 0.1443$, the three agreeing within 1.3 ± 0.5% seed by seed. **[M]** This viscous damping grows as k^z with $z = 2.15 \pm 0.10$, 2.03 ± 0.14 and 1.87 ± 0.12: a damped sound mode, not diffusion. **[M]** The stride stays within 1% of c_0 for $k \lesssim 0.9$ and rises toward the zone edge, by up to 16% along $\langle 100 \rangle$; at equal k up to 0.91, wavelengths down to 7 cells, the three strides agree within 1%. **[M]** The damping is anisotropic: at $k \approx 0.9$, Γ/k^2 is 0.017, 0.009 and 0.005 cell^2 per tick along the three directions, ordered as $\sum_a \hat{k}_a^4 - 1/3$, and the mixing among the route families, with mixing time 0.57–0.61 tick, gives this cubic form with the right sign and its size within 20%. **[I+M]** As $k \to 0$ the damped-wave model fitted to the modes turns the mode into diffusion, exponent 2, but the k^2 law is not observed: the fitted modes lie at wavenumbers 3 to 25 times the inverse of the fitted damping length, above the diffusive range, and D_N moves by up to about 20% between 24-, 32- and 48-cell tori, with no monotonic trend. **[I]** On random test patterns (32-cell torus, three seeds) the decay rate $\Gamma = c_0^2/D_N$ follows the fitted form $\Gamma = 0.118\,p\,(1 + 5.76\,p)$ for $p \geq 0.05$ and is superlinear above $p = 0.1$ at all three sizes, with local slopes 1.5–1.9; between 0.05 and 0.1, on the 32-cell torus only, the slope 1.27 is not significantly above 1, and the 24- and 48-cell tori, fitted on two modes, are not converged in size. **[M]**

Screening. The response falls off over ℓ to within 20% of the fitted ranges. **[M]** The units gap the operator independently, Δ lying within 8–37% of their number times one unit's gap; $\Delta \propto p^{1.07}$, so $\ell \propto p^{-0.54}$, with $\ell = 2.86$, 5.57 and 8.82 cells at $p = 0.109$, 0.0325 and 0.0137 (48-cell torus). **[M]** This reading came after the pre-registered fit, which favoured $\ell \propto 1/p$ through its lowest-density point, beyond the fitting window. **[M]** The class-signed phases $\pm\pi/3$ of the charge rule screen too, with ℓ 1.9 to 2.0 times longer at $p = 0.0325$. **[I+M]** At $\lambda = 0$ the response matches the operator at $p = 0$ to 2×10^{-11}. **[M]**

Identity. Since the 37 sets share their reference, a chi-square test with that covariance of the held contents gives 37.5 for 35 degrees of freedom. **[M]** Closures of 14 and 18 vertices, each with seven overtwisted vertices and $w = 1$, differ in adjacent A–B pairs and in held content by about 1.9% of an isolated overtwisted vertex, 0.27% of the closure's content, and are not identical. **[M]**

D.3 Readout runs

Two sources, one reader. Static seats write as in (I): in the count channel a release adds fewer than 0.04 captures at the other seat (two standard errors, two seeds), and in the charge channel the phase a seat gives a leaving bit is fixed by the pattern. **[F+M]** The excess of u_{12} over the value for independent visits, up to a factor 2.65 (two seeds), is path correlation between the seats, the reader's own phase contributing a factor 1 within errors; the shortest delay between two visits, 14 to 15 ticks, is one bit's travel along the shortest route, 14 edges at one edge per tick, against about 24 ticks for the collective mode over the same 3.5 cells. **[I+M]** With the sources fixed and only the reader's window varied, the share of u_{12} carried by bits that visited both seats within the window is 0.00–0.03 at 32 ticks, 0.23–0.43 at 64 and 0.72–0.85 at 128 (four configurations, six seeds each). **[M]** The first joint bit appears at windows of 28–37 ticks (means over six seeds), beyond the shortest joint path of 24,

j	μ	ν_{w}^{*}, $\varepsilon = 5\%$	ν_{w}^{*}, $\varepsilon = 1\%$	ξ, 5%	ξ, 1%	Holds	Ticks
1	0.508	6.35 ± 0.05	9.8 ± 0.2	0.738(13)	0.861(20)	11 268	15 987
2	0.252	12.65 ± 0.15	21.2 ± 0.4	0.897(16)	1.052(27)	16 345	33 588
3	0.1245	27.75 ± 0.60	48.95 ± 1.80	1.070(32)	1.269(48)	5326	17 266
$3'$	0.1245	25.90 ± 0.65	47.05 ± 2.05	0.993(34)	1.219(77)	2768	16 635
4	0.0627	60.95 ± 2.60	93.80 ± 6.55	1.234(22)	1.249(89)	1922	15 303
6	0.0156	242.6 ± 21.3	449.7 ± 89.0	1.255(51)	1.519(251)	766	25 888

Table 4: Kac runs, in reader steps ($\nu_{\mathsf{Kac}} = 1/\mu$); μ is the probability per step of the required configuration as measured in these hold runs, within 1.6% of 2^{-j}, the largest deviation at $j = 1$; 3 and $3'$ are two hold rules on three registers; $\xi = (\nu_{\mathsf{w}}^{*} - \nu_{\mathsf{d}})\,\mu/\ln(1/\varepsilon)$; ticks summed over the runs of each j; bootstrap standard errors, for ξ clustered over runs.

14 between the seats and 10 to the reader, and the share reaches a tenth of its full value at 44–52, in the same order in the four configurations, following the reader's distance to the seats. **[M]**

Dynamical readers and sources. In the transmission-line model a source moving at $\beta = 0.3$ and 0.5 shows $\mathcal{D}$ within 2% ahead of it, behind it and across its motion, against a static reference at 0.25%, beyond its 0.2% rule; the rate law is imposed on the source, so the model tests the factor $1/(1 + \beta\,\hat{n} \cdot \hat{u})$. **[M]** The model reproduces the co-moving case ($\beta = 0$) within 0.15%, 9 of 12 readers within 0.04%, short of its pre-registered 0.1% self-check, so the moving reader was not read and rests on the derivation. **[M]** With an injected source on a clean 40-cell torus, within seven cells the field times the rest-frame distance stays 1 to rms 0.0052 and the transverse-to-axial ratio is 1.151 against $\gamma = 1.155$ at $\beta = 0.5$ (Proposition 1), so (iii) holds to about 0.5% out to seven cells. At eight cells the ratio is 1.215 and the field ahead 0.892 of expectation. **[M]** Whether the box edge or the time window causes the eight-cell deviation is open. Through W_{tl} with references 20 cells from the path, $\sqrt{n_{+}n_{-}}/n_0$, with n_0 the count at rest, matches $\sqrt{1-\beta^2}$ at $\beta = 0.6$ within 0.8% along $\langle 100 \rangle$ and $\langle 111 \rangle$; the residual is lattice dispersion, the measured wavenumber exceeding ω/c_0 by 0.9–1.7% against 0.96% from a chain estimate. **[I+M]**

Kac window law. The runs behind Fig. 7 and Table 4 hold 64 seated closures with $w = 1$, a fixed test pattern, on a 16-cell torus, three seeds; a hold releases only when j gate registers match a required configuration; $\nu_{\mathsf{d}} = 2$. **[M]** From $\varepsilon = 5\%$ to 1%, ξ rises by a common factor 1.17 ± 0.02 (inverse-variance mean over j; $\chi^2 = 7.8$ for 5 degrees of freedom), the per-j ratios ranging from 1.01 ± 0.06 at $j = 4$ to 1.23 ± 0.05 at $j = 3'$. At both tolerances the window exceeds its value for independent steps by 3–53%. The law is this empirical bound at $\varepsilon \leq 5\%$, from runs of equal trigger count, 20 per seat (8 at $j = 6$), and 15 000 to 34 000 ticks per j. **[M]** On the floor of the Kac runs, the run with holds off, the CTM with 64 frozen closures on a 16-cell torus (three seeds of 3000 ticks), the joint probabilities of $j = 1$–4 and 6 registers show the averages and seat-by-seat deviations of Section 3: across seats μ varies with coefficient of variation 0.13–0.21, against 0.02–0.07 expected from sampling for $j \leq 4$ (0.14 at $j = 6$), a deviation fixed at each seat. **[I+M]** With only 766 holds, the $j = 6$ bound at 1% carries about 20% error. **[M]** Not yet run: a 32-cell torus, where an exponent below 0.7 or a size-dependent ξ would raise the CTM-correlation share, and full or mixed gate patterns, where ν_{w}^{*} following 2^j, not $1/\mu$, would refute the law.

Localization pilot. In a pilot on the machine, three identical seats exchanged by an exact threefold rotation read at $\lambda = 1/2$ as a symmetric mode and a degenerate doublet with no reader component, while at $\lambda = 0$ the same seats read as separate seats; with eight seeds the $\lambda = 1/2$ coupling behind this contrast is not resolved from zero (w142). **[M]** Breaking the identity localizes: with one seat's orientation changed, that seat reads as localized from a window of 4 ticks on, unchanged at longer windows. **[M]** Localization is set by detuning against coupling, here a detuning of about 20% against a coupling not resolved from zero; the window sets only the statistical resolution. **[I+M]** (Check D24.)

E Derivations

This appendix derives the readings of Section 8 keyed E and four results of Sections 5–7, none graded above the body.

Additivity at $\lambda = 0$. In the walk model a walker at a held register stays with probability κ_u per tick, the hold fraction at its vertex, and the routing is doubly stochastic; the runs set $\kappa_u = 1/2$ at every overtwisted vertex (Appendix C). A weight whose product with $1 - \kappa_u$ is uniform is mapped to itself, so the stationary weight is proportional to $1/(1 - \kappa_u)$ for every routing. Its excess over the CTM is the sum of $\kappa_u/(1 - \kappa_u)$ over registers, the held content, and no routing enters, so it does not depend on shape, closure length or w. The slope of $\mathcal{G}_0$ in its Laplace variable is this held content, by Little's law [44] held content times the clock. **[F]** The energy convention of Section 7 names it rest mass. **[R]** In the walk model the deviation from additivity is proportional to the killing rate (Section 5). **[M]**

Gauss identity. Summed over any region containing a closure, the resolvent equation makes the killing loss inside plus the net outflow equal to the total source. As the killing rate goes to zero the loss vanishes, so the flux is the same through every enclosing surface; a three-dimensional walk escapes and spreads isotropically, so the far field falls as $1/r$. **[F]** The network has no such law: frozen closures and conserved events give every conserved current zero mean flux through a closed surface, and the only quantity equal to $3w$ is the turning accumulated along a route. **[F]** A reader that encloses its source breaks the interchangeability of readers and sources of one kind, so no antenna reads an enclosing flux. **[R]**

Redshift. Between seated parties the channel is time-invariant in network ticks and the counts in flight stay bounded, so the factor out times the factor back is 1. Its reciprocal part is 1; the anti-reciprocal part is a ratio of two quantities, one at each seat, common to all arrivals from the source, so its logarithm is a difference of one function on seats. **[F]** Reading the reciprocal part as motion (Section 6) makes that difference a potential difference, composing as a redshift, not a velocity. **[R]**

Drift anisotropy. On the defect-free CTM each tick is a bijection that conserves N and every Q_R, so a product measure in which each register's occupancy is set by a common parameter plus a drift parameter times its velocity sign is stationary; at $\rho = 1/2$ the common parameter vanishes at any drift, N_a does not depend on the drift, and the occupancy on routes along $+a$ is the ρ_a of Eq. (4). **[F]** Given local equilibrium, reached by the axial number share within two ticks, number and lattice momentum obey $\partial_n N + \sum_a \partial_a \mathcal{P}_a = 0$ and $\partial_n \mathcal{P}_a + v_{\text{bit}}^2 \partial_a N_a = 0$, which linearized about this measure give Eq. (4), and at rest, with $N_a = N/3$, Eq. (3). For a drift βc_0 along a cube axis, Eq. (4) gives the strides along and across the drift as $c_\parallel^2 = c_0^2(1 - 3\beta^2)/(1 - \beta^2)$ and $c_\perp^2 = c_0^2/(1 - \beta^2)$. **[F+M]** At $\beta = 0.2668$ the machine gives $0.920\, c_0$ along (0.920 predicted) and $1.037\, c_0$ across (1.038); at $\beta = 0.4397$, 0.72–0.73 (0.722) and 1.110 (1.113). **[M]** A drift is a motion of the causal flow over the graph, not of the CTM, which rests with the pattern that damps it (Section 5); it serves here only to test Eq. (4) at Euler order (cf. [45]). **[R+M]**

Rate law. For dynamical readers and sources, read as moving relative to the CTM with signals at an isotropic c_0, let a party's ordinal advance at some fraction of its rest rate; a seated reader and a source receding at β then exchange the factor $1 - \beta$ over that fraction out and the fraction over $1 + \beta$ back. Radar reciprocity sets them equal, so the fraction is $\sqrt{1 - \beta^2} = 1/\gamma$. **[R]** With every dynamical party on this law, proper counts and radar give a seated reader the factor $\mathcal{D}$ of Proposition 1. **[R]**

Coulomb measure. The limit $\omega \to 0^+$, taken in W_{tl}, is the low-frequency end of a time-resolved reading, while W_{id} is the stationary measure at $\omega = 0$. **[R]** For a source at rest both reduce to one Poisson problem, a constant factor apart. **[F]** For a dynamical source the quasi-static condition holds everywhere under the transmission-line kernel, since $\omega r/c_0 \approx \beta$, but under the diffusive kernel of W_{id} only near the source, so kinematic readings belong to W_{tl} (Section 7). **[R+M]**

Kac window law. For a stationary, ergodic sequence, Kac's lemma gives a configuration of probability μ per step the mean return time $1/\mu$. **[F]** For independent steps a window misses the event with probability $(1-\mu)^{\nu_{\mathsf{w}}}$, so missing it at most with probability ε needs $\nu_{\mathsf{w}} \geq \ln(1/\varepsilon)/\ln\bigl(1/(1-\mu)\bigr) \approx \nu_{\mathsf{Kac}} \ln(1/\varepsilon)$, plus the shortest hold: Eq. (5) with $\xi = \mu/\ln\bigl(1/(1-\mu)\bigr)$, 0.72 at $j=1$ and 0.99 at $j=6$. **[F]** The CTM's joint probabilities, within 1.1% of 2^{-j} on average (Section 3), let joint reads multiply their return times as Section 7 uses. **[M]** A counting-noise window, growing as ε^{-2}, would make the 1% window 25 times the 5% one; measured: 1.54–1.85 (Table 4). **[M]**

Readout cosmology. Readout light runs at c_0 in bands per network tick at every n, and with its speed fixed in reader units one conformal factor serves every unit. So n reads as conformal time η, a reader cell is b network cells on a side, reader time is $dt = d\eta/b$, the scale factor is $1/b$ and $H = -db/d\eta$. **[R]** Held content sits at unmoving overtwisted vertices and adds over them, so a reader cell's held content scales as b^3. **[R]** In the continuum limit, substituting $1/b$ into the conformal Friedmann equation of general relativity, with matter, a constant and $k=0$ from the flat T^3, gives $(db/d\eta)^2 = \mathcal{C}_\Lambda + \mathcal{C}_{\mathsf{m}} b^3$; the law read is its derivative $b'' = \frac{3}{2}\mathcal{C}_{\mathsf{m}} b^2$, which holds no $\mathcal{C}_\Lambda$, a first integral, and $(1/b)'' = \frac{1}{2}\mathcal{C}_{\mathsf{m}} + 2\mathcal{C}_\Lambda b^{-3} > 0$. Anything counted per network cell scales as b^3 per reader cell and joins $\mathcal{C}_{\mathsf{m}}$, so the held level enters $\mathcal{C}_\Lambda$ only as a share. **[R]** Since $H = -db/d\eta > 0$ and $(1/b)'' > 0$, with $\mathcal{C}_\Lambda = 0$ too, $1/b$ is increasing and convex in η; such a curve never saturates, so it is not the bounded mixed fraction. **[R]**

In the continuum limit, when $\mathcal{C}_{\mathsf{m}} b^3 \ll \mathcal{C}_\Lambda$, $-db/d\eta \to \sqrt{\mathcal{C}_\Lambda} \equiv H_\Lambda$, so $b = H_\Lambda(\eta_\infty - \eta)$ and $H_\Lambda^{-1} = (\eta_\infty - \eta)/b$, the remaining network ticks in reader ticks. With $dt = d\eta/b$, $b \propto \exp(-H_\Lambda t)$, so $H^2 - H_\Lambda^2 = \mathcal{C}_{\mathsf{m}} b^3 \propto \exp(-3H_\Lambda t)$ to leading order, with constant $H = H_\Lambda$, de Sitter, as fixed point. The knee $\mathcal{C}_{\mathsf{m}} b^3 = \mathcal{C}_\Lambda$ is $H^2 = 2H_\Lambda^2$, the matter–Λ equality. **[R]** If a reader tick is at least one machine step, a network tick (Section 8.5), b cannot fall below 1 and stops, so the conformal future is unbounded. **[R]** Under this premise the continuum equation fails where b stops, since $\mathcal{C}_\Lambda > 0$ forbids $b' = 0$. **[R]** If Newton's constant G is a number times a cell area (Section 8.5), a network cell's area in reader units scales as b^{-2}, so with $dt = d\eta/b$ a network cell would make $d\ln G/dt = 2H$. **[Cond]**

Bunching in a resolution cell. Let a resolution cell hold M independent modes of mean intensity $\bar{I}$, each counted as Poisson at given intensity (Section 7), and let n_{c} be the cell's count. For the collective mode, a nearly Gaussian sum, each intensity I_i is exponential, $\langle I_i^2 \rangle = 2\bar{I}^2$, so $\langle n_{\mathsf{c}}(n_{\mathsf{c}}-1)\rangle = \langle (\sum_i I_i)^2 \rangle = M(M+1)\bar{I}^2$ and $g^{(2)}(0) = \langle n_{\mathsf{c}}(n_{\mathsf{c}}-1)\rangle / \langle n_{\mathsf{c}}\rangle^2 = 1 + 1/M$. **[F]** For M single sites, each a register holding 1 with probability ρ, only distinct sites pair, $\langle n_{\mathsf{c}}(n_{\mathsf{c}}-1)\rangle = M(M-1)\rho^2$, and $g^{(2)}(0) = 1 - 1/M$. **[F]**

F Notation

Table 5 lists the symbols that recur, that this paper introduces, or that it uses in a sense of its own; standard symbols in their usual sense are defined where they appear.

Symbol	Meaning	§
Network: structure and machine		
T^3; A, B	the three-torus; the two vertex classes	2
n	network tick, a local causal ordinal	2
ρ	occupancy, the fraction of registers holding 1	2
s; u, u'	side of a band; a vertex; the ends of a band	3, B
e	a band	3
χ; χ_0, χ_1	strand label $s \oplus [u \in \mathrm{B}]$; the two strands	3
Υ	handedness of the lock's half twists, ± 1	3
τ_e	number of half twists on band e	3
f_u; rot_u; g_e	overtwist bit; rotation-system bit; routing bit	B, C
p	density of overtwisted vertices	5
w	closure index, the turning number of a closed route	4
h; q	band-rotation sign, read as helicity; route-charge sign, read as charge sign	4
q_{src}, q_{rdr}	charge signs of source and reader	8
λ; θ	phase weight, read as spin weight; turning angle $\pm 2\pi/3$	4
N; Q	number density; strand-difference density	5
R; Q_R, K_R	a route; its two route charges	5
a, a'	cube-axis indices	5
v_{bit}; c_0	bit stride; collective-mode stride $v_{\mathrm{bit}}/\sqrt{3}$	1, 5
$\mathcal{G}_\lambda$	walk sum over killed walks	5
D_N	diffusion constant of N	D
Γ	decay rate of the collective mode, viscous damping at $p = 0$, c_0^2/D_N from the sinks at $p > 0$	5, D
ℓ; Δ; D_{tl}	screening length; gap of the static flux-floor operator; its stiffness at $p = 0$	5
Φ	phase per overtwisted vertex	5
Operations and read-as names		
t_{bc}	body-centre translation, exchanging A and B	2
Rot_4; Rot_2	fourfold screw rotation; twofold rotation	2; 4
Mir; Inv; σ_d	reversed rotation system; inversion; diagonal mirror $\mathrm{Inv} \circ \mathrm{Rot}_2$	4
$\mathcal{U}$	the update	4
X	complement, $0 \leftrightarrow 1$ in every register	2
J_{hist}; J_{state}	causal reversal; state reversal	2
C, P, T	read-as names of t_{bc}, σ_d, J_{state}	7
Readout		
o; $\mathcal{S}_o$; $\hat{n}$	a reader; its sky; a direction on it	6
β	speed in units of c_0, in Appendix E also a drift	6
ν	the reader's own ordinal	6
ω; $\overline{h}$	demodulation frequency; reduced Planck constant	1; 7
W_{tl}, W_{id}	transmission-line and identity walk measures	6
$\mathcal{R}$, $\mathcal{K}$; u_{12}	reader's demodulation, propagation along relay chains; relay-composed cross term	6
n_{c}, $\bar{n}_{\mathrm{c}}$	count of a cell, its mean	7
E_+	C-even part of the compared cross reading	8
Kac window law		
j; μ; ν_{Kac}	registers read jointly; probability per reader step; return time $1/\mu$	7
ε; $\xi(j)$	tolerance of a window; prefactor of the law	7
ν_{w}	window length	7
Cosmology		
b	reader tick length in network ticks	8
$\mathcal{C}_\Lambda$, $\mathcal{C}_{\mathrm{m}}$; Λ	constants of the readout Friedmann equation; the cosmological constant, a first integral	8

Table 5: Symbols and the section or appendix that defines them.

Data and code availability

The code release runs the machine of Appendix C and the checks of Appendix D; it needs Python 3.11 or later, NumPy and SciPy. The checks and the run records they read are in the deposit doi:10.5281/zenodo.23663592; the records are listed with their SHA-256 hashes. A README in the deposit maps every check key to its check module, its producers and its records.

Acknowledgments

The author thanks the community of theoretical physicists and mathematicians on whose concepts this construction is built. The picture the author keeps returning to is the elephant in a dark room: the programs that look beneath spacetime each hold something that is really there, and the difficulty is the dark. This paper borrows their abstractions, those Section 10 names, and reassembles them by physical intuition into one machine, trying to set each piece at the level where it belongs and to find what is still missing between them.

The author thanks Anthropic for the AI tools used here, the Claude Opus and Fable series.

Author Contributions

The human author holds the picture and its intuition, the ontological choices and the outermost decisions, taken at checkpoints: scope, title, tone and the frame of the readings. A nested team of Claude agents unfolds that picture and its tasks layer by layer: an integrating session holds the middle layer, the rulings and the specification, and agents with their own context hold details and implementation. In research the team alternated breadth, widening the map, with depth, carrying candidates to a checkable end; it implemented and ran the machine, derived results, audited claims against the machine's readouts and retrieved mathematics and physics, and it proposed candidates, which the author accepted, revised or rejected. In writing, a Writer held the text, an Editor checked it, cold-read sessions, without the project's context, read the drafts, and the integrating session ruled. Claude models also corrected English grammar and wording, improved fluency, drew the figures and edited the LaTeX source. The human author reviewed all AI-generated content and takes full responsibility for the published article.

References

[1] K. Zuse, *Rechnender Raum*, Schriften zur Datenverarbeitung, Vol. 1 (Vieweg, Braunschweig, 1969).

[2] E. Fredkin, Digital mechanics: an informational process based on reversible universal cellular automata, *Physica D* **45**, 254–270 (1990).

[3] C. Barceló, S. Liberati and M. Visser, Analogue gravity, *Living Rev. Relativ.* **14**, 3 (2011).

[4] H. S. M. Coxeter, On Laves' graph of girth ten, *Canad. J. Math.* **7**, 18–23 (1955).

[5] M. O'Keeffe, M. A. Peskov, S. J. Ramsden and O. M. Yaghi, The Reticular Chemistry Structure Resource (RCSR) database of, and symbols for, crystal nets, *Acc. Chem. Res.* **41**, 1782–1789 (2008).

[6] A. F. Wells, *Three-Dimensional Nets and Polyhedra* (Wiley, New York, 1977).

[7] T. Sunada, Crystals that nature might miss creating, *Notices Amer. Math. Soc.* **55**, 208–215 (2008).

[8] J. Hardy, Y. Pomeau and O. de Pazzis, Time evolution of a two-dimensional model system. I. Invariant states and time correlation functions, *J. Math. Phys.* **14**, 1746–1759 (1973).

[9] U. Frisch, B. Hasslacher and Y. Pomeau, Lattice-gas automata for the Navier–Stokes equation, *Phys. Rev. Lett.* **56**, 1505–1508 (1986).

[10] G. Călugăreanu, L'intégrale de Gauss et l'analyse des nœuds tridimensionnels, *Rev. Math. Pures Appl.* **4**, 5–20 (1959).

[11] J. H. White, Self-linking and the Gauss integral in higher dimensions, *Amer. J. Math.* **91**, 693–728 (1969).

[12] F. B. Fuller, The writhing number of a space curve, *Proc. Natl. Acad. Sci. USA* **68**, 815–819 (1971).

[13] H. Bondi, *Relativity and Common Sense* (Anchor Books, Doubleday, Garden City, N.Y., 1964).

[14] A. Einstein, Zur Elektrodynamik bewegter Körper, *Ann. Phys.* **17**, 891–921 (1905).

[15] S. Chadha and H. B. Nielsen, Lorentz invariance as a low energy phenomenon, *Nucl. Phys. B* **217**, 125–144 (1983).

[16] L. Bombelli, J. Henson and R. D. Sorkin, Discreteness without symmetry breaking: a theorem, *Mod. Phys. Lett. A* **24**, 2579–2587 (2009).

[17] M. Kac, On the notion of recurrence in discrete stochastic processes, *Bull. Amer. Math. Soc.* **53**, 1002–1010 (1947).

[18] T. D. Lee, A theory of spontaneous T violation, *Phys. Rev. D* **8**, 1226–1239 (1973).

[19] S. O. Bilson-Thompson, A topological model of composite preons, arXiv:hep-ph/0503213 (2005).

[20] D. Finkelstein and J. Rubinstein, Connection between spin, statistics, and kinks, *J. Math. Phys.* **9**, 1762–1779 (1968).

[21] P. Ehrenfest and J. R. Oppenheimer, Note on the statistics of nuclei, *Phys. Rev.* **37**, 333–338 (1931).

[22] T. Jeltes, J. M. McNamara, W. Hogervorst, W. Vassen, V. Krachmalnicoff, M. Schellekens, A. Perrin, H. Chang, D. Boiron, A. Aspect and C. I. Westbrook, Comparison of the Hanbury Brown–Twiss effect for bosons and fermions, *Nature* **445**, 402–405 (2007).

[23] H. Rauch, A. Zeilinger, G. Badurek, A. Wilfing, W. Bauspiess and U. Bonse, Verification of coherent spinor rotation of fermions, *Phys. Lett. A* **54**, 425–427 (1975).

[24] S. A. Werner, R. Colella, A. W. Overhauser and C. F. Eagen, Observation of the phase shift of a neutron due to precession in a magnetic field, *Phys. Rev. Lett.* **35**, 1053–1055 (1975).

[25] A. Einstein, Zum gegenwärtigen Stande des Strahlungsproblems, *Phys. Z.* **10**, 185–193 (1909).

[26] H. Wielandt, Unzerlegbare, nicht negative Matrizen, *Math. Z.* **52**, 642–648 (1950).

[27] M. Henneaux and C. Teitelboim, The cosmological constant and general covariance, *Phys. Lett. B* **222**, 195–199 (1989).

[28] W. G. Unruh, Unimodular theory of canonical quantum gravity, *Phys. Rev. D* **40**, 1048–1052 (1989).

[29] S. Weinberg, The cosmological constant problem, *Rev. Mod. Phys.* **61**, 1–23 (1989).

[30] G. Spencer-Brown, *Laws of Form* (Allen and Unwin, London, 1969).

[31] T. Toffoli and N. Margolus, *Cellular Automata Machines: A New Environment for Modeling* (MIT Press, Cambridge, MA, 1987).

[32] G. 't Hooft, *The Cellular Automaton Interpretation of Quantum Mechanics* (Springer, Cham, 2016).

[33] R. Landauer, Irreversibility and heat generation in the computing process, *IBM J. Res. Dev.* **5**, 183–191 (1961).

[34] M. Z. Guo, G. C. Papanicolaou and S. R. S. Varadhan, Nonlinear diffusion limit for a system with nearest neighbor interactions, *Commun. Math. Phys.* **118**, 31–59 (1988).

[35] G. Gallavotti, Divergences and the approach to equilibrium in the Lorentz and the wind-tree models, *Phys. Rev.* **185**, 308–322 (1969).

[36] C. Boldrighini, L. A. Bunimovich and Ya. G. Sinai, On the Boltzmann equation for the Lorentz gas, *J. Stat. Phys.* **32**, 477–501 (1983).

[37] J. A. Wheeler, Information, physics, quantum: the search for links, in *Complexity, Entropy, and the Physics of Information*, edited by W. H. Zurek (Addison-Wesley, Redwood City, CA, 1990), pp. 3–28.

[38] C. W. Misner, K. S. Thorne and J. A. Wheeler, *Gravitation* (Freeman, San Francisco, 1973), Chap. 44.

[39] R. Penrose, Angular momentum: an approach to combinatorial space-time, in *Quantum Theory and Beyond*, edited by T. Bastin (Cambridge University Press, Cambridge, 1971), pp. 151–180.

[40] L. Bombelli, J. Lee, D. Meyer and R. D. Sorkin, Space-time as a causal set, *Phys. Rev. Lett.* **59**, 521–524 (1987).

[41] S. Wolfram, A class of models with the potential to represent fundamental physics, *Complex Syst.* **29**, 107–536 (2020).

[42] T. Konopka, F. Markopoulou and S. Severini, Quantum graphity: a model of emergent locality, *Phys. Rev. D* **77**, 104029 (2008).

[43] J. A. Ellis-Monaghan and I. Moffatt, *Graphs on Surfaces: Dualities, Polynomials, and Knots* (Springer, New York, 2013).

[44] J. D. C. Little, A proof for the queuing formula $L = \lambda W$, *Oper. Res.* **9**, 383–387 (1961).

[45] U. Frisch, D. d'Humières, B. Hasslacher, P. Lallemand, Y. Pomeau and J.-P. Rivet, Lattice gas hydrodynamics in two and three dimensions, *Complex Syst.* **1**, 649–707 (1987).